BRNO UNIVERSITY OF TECHNOLOGY
VYSOKÉ UČENÍ TECHNICKÉ V BRNĚ

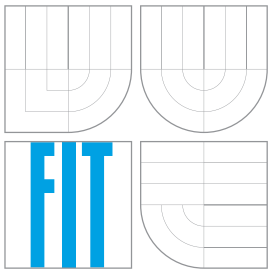

FACULTY OF INFORMATION TECHNOLOGY
DEPARTMENT OF INTELLIGENT SYSTEMS
FAKULTA INFORMAČNÍCH TECHNOLOGIÍ
ÚSTAV INTELIGENTNÍCH SYSTÉMŮ

GENERATION OF SKIN DISEASE INTO THE SYNTHETIC FINGERPRINTS

GENEROVÁNÍ ONEMOCNĚNÍ KŮŽE DO SYNTETICKÝCH OTISKŮ PRSTŮ

MASTER'S THESIS
DIPLOMOVÁ PRÁCE

AUTHOR Bc. MILAN BÁRTA
AUTOR PRÁCE

SUPERVISOR doc. Ing., Dipl.-Ing. MARTIN DRAHANSKÝ, Ph.D.
VEDOUCÍ PRÁCE

BRNO 2016

Vysoké učení technické v Brně - Fakulta informačních technologií

Ústav inteligentních systémů Akademický rok 2015/2016

Zadání diplomové práce

Řešitel: **Bárta Milan, Bc.**
Obor: Bioinformatika a biocomputing
Téma: **Generování onemocnění kůže do syntetických otisků prstů**
Generation of Skin Disease into the Synthetic Fingerprints
Kategorie: Zpracování obrazu

Pokyny:

1. Prostudujte literaturu týkající se biometrického rozpoznávání otisků prstů, onemocnění kůže na prstech a generování syntetických otisků prstů.
2. Z dostupné databáze ve skupině STRaDe na FIT VUT v Brně zvolte jedno až dvě nejčetnější onemocnění kůže na prstech.
3. Navrhněte algoritmus úpravy syntetického otisku prstu zanesením změn napodobujících onemocnění kůže dle výběru z bodu 2.
4. Vámi navržený postup z předchozího bodu implementujte.
5. Proveďte vygenerování minimálně 100 syntetických otisků prstů s výše uvedeným poškozením. S těmito syntetickými otisky prstů proveďte experimenty (např. stanovení kvality otisku prstu, porovnání s nepoškozenými syntetickými otisky prstů).
6. Dosažené výsledky shrňte a diskutujte dopad vlivu onemocnění kůže na rozpoznávání otisků prstů.

Literatura:

- DRAHANSKÝ Martin, ORSÁG Filip a DOLEŽEL Michal et al. *Biometrie*. Brno: Computer Press, s.r.o, 2011. ISBN 978-80-254-8979-6.
- SFinGe (Synthetic Fingerprint Generator) - *biolab.csr.unibo.it/sfinge.html*.
- CHALOUPKA Radek. *Generátor otisků prstů*. DP, FIT VUT v Brně, 2007, s. 52.
- HABIF Thomas P. *Clinical dermatology*. Fifth Edition, Elsevier, 2010, p. 1101, ISBN 978-0-7234-3541-9.

Při obhajobě semestrální části projektu je požadováno:

- Body 1 až 3.

Podrobné závazné pokyny pro vypracování diplomové práce naleznete na adrese http://www.fit.vutbr.cz/info/szz/

Technická zpráva diplomové práce musí obsahovat formulaci cíle, charakteristiku současného stavu, teoretická a odborná východiska řešených problémů a specifikaci etap, které byly vyřešeny v rámci dřívějších projektů (30 až 40% celkového rozsahu technické zprávy).

Student odevzdá v jednom výtisku technickou zprávu a v elektronické podobě zdrojový text technické zprávy, úplnou programovou dokumentaci a zdrojové texty programů. Informace v elektronické podobě budou uloženy na standardním nepřepisovatelném paměťovém médiu (CD-R, DVD-R, apod.), které bude vloženo do písemné zprávy tak, aby nemohlo dojít k jeho ztrátě při běžné manipulaci.

Vedoucí: **Drahanský Martin, doc. Ing., Dipl.-Ing., Ph.D.**, UITS FIT VUT
Datum zadání: 1. listopadu 2015
Datum odevzdání: 25. května 2016

VYSOKÉ UČENÍ TECHNICKÉ V BRNĚ
Fakulta informačních technologií
Ústav inteligentních systémů
612 66 Brno, Božetěchova 2

doc. Dr. Ing. Petr Hanáček
vedoucí ústavu

Abstract

The thesis deals with design and implementation of a tool for simulating marks of chosen skin diseases into a synthetic fingerprint. The diseases selected to work with are warts and atopic eczema. The marks of diseases are generated into a synthetic fingerprint image created by the SFinGe application. Existing disesase-affected fingerprints from the STRaDe database are analysed in detail. Then, methods for simulating the diseases into a synthetic fingerprint are proposed, implemented, and the results are evaluated.

Abstrakt

Diplomová práce se zabývá návrhem a implementací nástroje, s jehož pomocí je možné simulovat stopy konkrétních onemocnění kůže v umělém otisku prstu. Vybraná onemocnění pro tuto práci jsou bradavice a atopický ekzém. Generování známek onemocnění probíhá do umělého otisku vytvořeného aplikací SFinGe. Existující otisky prstů s onemocněním z databáze STRaDe jsou analyzovány, následně jsou navrženy postupy pro simulaci konkrétních onemocnění do umělého otisku prstu, ty jsou implementovány a výsledek je vyhodnocen.

Keywords

Biometry, fingerprint, synthetic fingerprint, SFinGe, skin diseases, warts, atopic dermatitis, eczema

Klíčová slova

Biometrie, otisk prstu, umělý otisk prstu, SFinGe, kožní onemocnění, bradavice, atopický ekzém, ekzém

Reference

BÁRTA, Milan. *Generation of Skin Disease into the Synthetic Fingerprints.* Brno, 2016. Master's thesis. Brno University of Technology, Faculty of Information Technology. Supervisor Drahanský Martin.

Generation of Skin Disease into the Synthetic Fingerprints

Declaration

Herewith I declare that I have written my final thesis by myself under the supervision of doc. Ing., Dipl.-Ing. Martin Drahanský, Ph.D.

I used only sources mentioned in the Bibliography section.

.....
Milan Bárta
May 23, 2016

Acknowledgements

I would like to express my gratitude to my supervisor doc. Ing., Dipl.-Ing. Martin Drahanský, Ph.D., for the useful comments, remarks and guidance through the learning process of this master thesis.

Contents

List of Figures

List of Tables

Chapter 1

Introduction

Fingerprint recognition is one of the most often used biometric technologies all over the world. Nowadays, users find it even on their mobile phones. It has been designed so that everyone can use it. However, a problem rises in case of people with some kind of skin disease, disallowing them to use fingerprint scanning technology in order to authenticate themselves.

Skin diseases represent an important issue in fingerprint recognition. Unfortunately, this problem is often not taken into consideration when designing such a device. Although precise numbers are hard to calculate, it is estimated that 20–25% of people suffer from some kind of skin disease [8]. With such a large number of potential users of fingerprint technology, scanning techniques should be ready to deal with certain effects that the diseases have on the ridge structure of disease-affected fingerprints.

This requirement leads to a larger demand on testing of the recognition algorithms. However, large databases of fingerprints are required in order to perform such tests. It is also a very time-consuming task, as many people need to participate in order to acquire enough samples. In order to overcome these problems, a database of synthetic fingerprints can be used. With already existing tools, a large quantity of synthetic fingerprints can be generated in a short amount of time. However, fingerprint images produced by synthetic fingerprint generating tools are often too perfect to be used for any meaningful testing of existing algorithms.

Therefore, this thesis aims to alter the generated synthetic fingerprints, so that they appear as fingerprints from people suffering from various selected skin diseases. Using a database of altered fingerprint images, existing algorithms might be better prepared for users that suffer from such diseases than they are now.

The thesis is divided into several chapters, first of them being this introduction chapter. Chapter 2 introduces the reader to the thesis main subject and explains terms that are required to be understood in order to fully comprehend the studied problem. The proposed solution to the problem is presented in chapter 3 together with deeper analysis of the selected diseases to simulate. A description of an algorithm modifying a synthetic fingerprint in a similar way as the selected disease would is presented as well. Implementation details and description of tools and libraries used can be found in chapter 4. The resulting outputs of the implemented system can be found at the end of this chapter too. The generated fingerprint images have been subjected to experiments. They have been conducted in order to verify the degree of damage caused by the simulated disease and also to assess their quality features before and after the simulation. The methodology of conducted experiments and their results can be found in chapter 5. The results are concluded in the final chapter 6.

Chapter 2

Fingerprint biometrics in relation to skin diseases

In order to understand the topic of fingerprint biometrics in relation to skin diseases, several crucial terms have to be explained and important subjects explored.

In this chapter, section 2.1 introduces reader into the field of research exploring biometrics and explains the functionality of a biometric system. In section 2.2, a fingerprint structure is introduced, fingerprint classification system explained, and singularities of a fingerprint listed and described. Section 2.3 describes various methods and techniques of fingerprint acquisition. Fingerprint recognition process is explained in detail in section 2.4. An important part of this thesis deals with synthetic fingerprints. The ways of creating one are described in section 2.5. Finally, section 2.6 deals with various skin diseases that affect the way fingerprint acquisition works.

2.1 Biometrics

Biometrics [9] is a science of establishing the identity of an individual based on the physical, chemical or behavioural features. The first reliable evidence of using biometric features in order to identify a person is from the 19^{th} century. The first pioneers in biometric recognition technology were anthropometry, based on finding measures of several physical features that stay rather constant over the life, and fingerprint recognition. [9]

Biometrics plays an irreplaceable role in identification management systems that have gained on importance in everyday life of each of us, especially in the last few decades. A crucial task in an identification management system is the determination of an individual's identity. Traditional methods of identity verification include knowledge-based (e.g., passwords) and token-based (e.g., ID cards) mechanisms. However, these can be easily lost, stolen or modified, therefore compromising the security of accessed system. Biometrics provides a natural and reliable solution to overcome the deficiencies of previously mentioned mechanisms by utilizing automated schemes to individual recognition based on their biological characteristics. [12]

Biometric systems [13] utilize a large variety of physical and behavioural features, including fingerprint, hand geometry and vain, face, iris, retina, voice pattern, signature or the DNA information of individual in order to establish their identity. While biometric systems have their own limitations, they often outperform traditional security methods by not being possible to steal them or share them with other system users. Besides increasing security levels, biometric systems also provide users with higher comfort and convenience.

2.1.1 Biometric system

A biometric system is basically a pattern recognition system [13]. Its task is to recognise a person based on the authenticity of a specific physiological or behavioural feature possessed by that person. The recognition process includes biometric data acquisition, extracting a salient feature set from the data, comparison of the extracted feature set against the one(s) stored in the database of the biometric system, and execution of an action based on the result of comparison. [13]

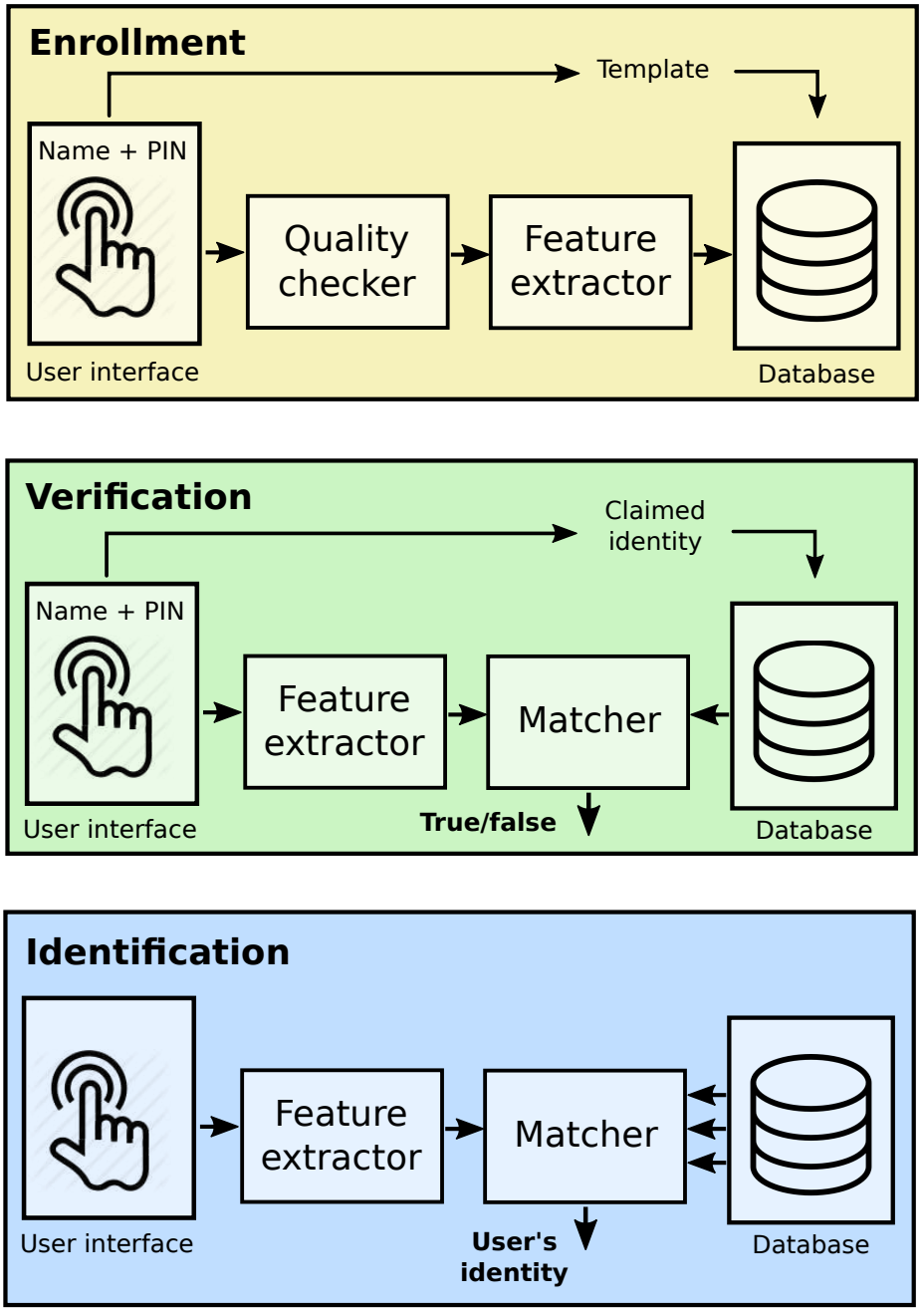

Figure 2.1: Enrolment, verification, and identification in a biometric system [18].

Depending on the application context, a biometric system may be called either a verification system or an identification system (see figure 2.1) [12]. A verification system validates a person's identity by comparing the captured biometric data with their own template already existing in the system database. In this case of recognition, a user claims an identity (e.g., by user name or ID) and the system makes a comparison in order to determine if the claim is true or not.

In the identification system mode, the biometric system recognises an individual by looking them up in its database of templates of all the users enrolled in the system. Therefore, in order to establish an individual's identity, the system conducts one-to-many comparison. This kind of recognition does not require a user to claim an identity. [12]

2.1.2 Biometric characteristics

Any human biometric characteristic can be used as a biometric identifier to recognise an individual as long as it satisfies the requirements defined by Jain et al. [13]. The requirements specify the suitability of a physical or a behavioural trait to be used in a biometric application. They include:

- **universality:** every individual using the system should possess the trait;
- **uniqueness:** the given trait should sufficiently differ among population;
- **permanence:** the biometric trait should be sufficiently invariant over a period of time. A trait that changes significantly over an individual's lifetime is not considered a useful biometric;
- **measurability:** it should be possible to acquire the biometric trait and store it in digital; form using suitable devices. Furthermore, the acquired raw data should be amendable to processing in order to extract feature sets from them;
- **performance:** the recognition accuracy and the resources required should meet the constraints for given application;
- **acceptability:** individuals that will use the application should be willing to present their biometric traits to the system;
- **circumvention:** this describes the ease with which the trait can be imitated by an imposter.

2.2 Fingerprint biometrics

Fingerprints have been used for personal identification for many decades and their matching accuracy has been found to be very high. It has been empirically determined that the fingerprints of identical twins are different and so are the prints on each finger of the same person [22]. However, fingerprints of a small fraction of population might be unsuitable for automatic identification because of genetic factors, ageing, diseases or environmental and occupational reasons (cuts and bruises on fingerprints of manual workers).

2.2.1 Fingerprint

A fingerprint is a representation of a pattern created by epidermis consisting of interleaved ridges and valleys. Epidermis is the topmost layer constituting skin, together with dermis (true skin) and subcutaneous (fat) layer (see figure 2.2) [8].

Fingerprint ridges form through a combination of genetic and environmental factors in a process similar to the growth of capillaries and blood vessels in angiogenesis. The genetic

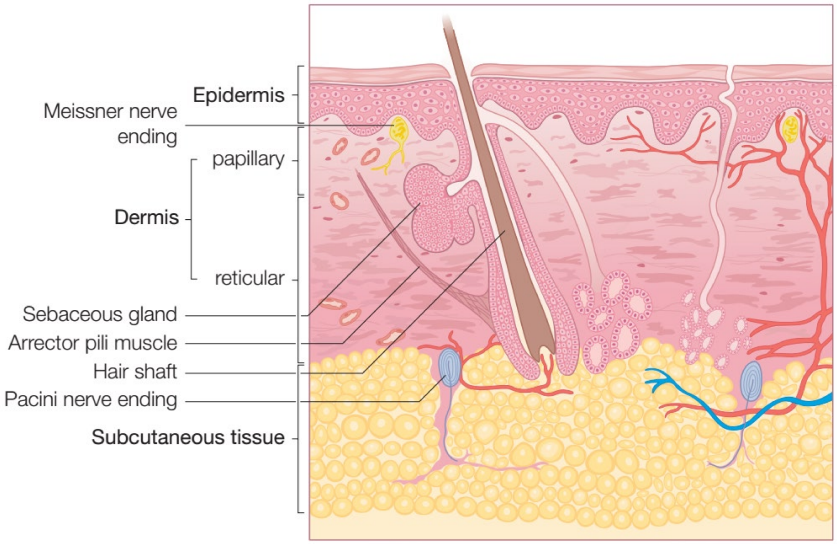

Figure 2.2: Skin structure [15].

code gives general instructions on the way skin should be formed, however the specific way it forms is a result of random effects on the child during its development in womb. This is why fingerprints of identical twins are always different too. The fingerprint formation finishes at about seventh month of unborn child development and the ridge configurations are permanent throughout the life of an individual [12, 22]. This makes fingerprints an ideal biometric feature for recognition.

In a typical case, in a fingerprint image, ridges are dark lines whereas valleys are bright (see figure 2.3). Width of ridges varies from 100 µm to 300 µm. The period of ridge/valley cycle is around 500 µm. Injuries usually do not affect the underlying ridge structure, thus the original pattern often emerges once new skin regrows. [13]

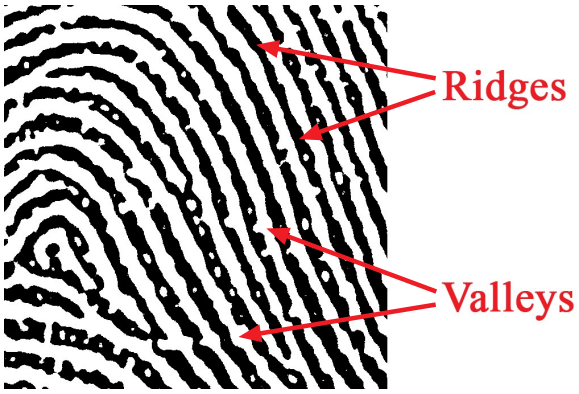

Figure 2.3: Ridges and valleys on a fingerprint image.

2.2.2 Fingerprint classification

Ridges and valleys usually run in parallel. However, sometimes they terminate or bifurcate, and by doing so, specific fingerprint structures are created. From a global point of view, the fingerprint pattern consists of one or more regions of distinctive shape with high frequency

of terminations or particular curvature. These regions are called singularities. [19]

Some fingerprint matching techniques recognise a centre point called *core* and a *delta* in order to easily align two fingerprints at the global level (see figure 2.4). However, the distinctiveness of them alone is not sufficient for accurate matching. [13]

In practice, the core is defined as the centre of the northernmost loop type singularity. It is however difficult to find a core in fingerprints that contain no loop at all (e.g., fingerprints belonging to the arch class). In this case, core is defined as the point of maximum ridge line curvature. Delta is the centre of triangular regions where three different direction flows meet. [16, 1]

Figure 2.4: Core and delta located on a particular fingerprint image.

Singular regions are often used as the top-level fingerprint classification feature. The goal of dividing fingerprint images into a predefined set of classes is to simplify search and their retrieval. The categories are: *left loop*, *right loop*, *whorl*, *arch*, and *tended arch* (see figure 2.5). [13]

2.2.3 Fingerprint minutiae

At the local level, fingerprint can be described by other features, called minutiae [13]. Minutia means small detail and in fingerprint, they describe the way ridge can be discontinued. Two most commonly used types of ridge discontinuation are *termination* (ridge comes to an end suddenly) and *bifurcation* (ridge is divided into two). Although several different types can be distinguished (see figure 2.6), only a small subset of the whole minutiae list is commonly used in practice because of increasing difficulty in automatically discerning the different types of minutiae with required accuracy. [13]

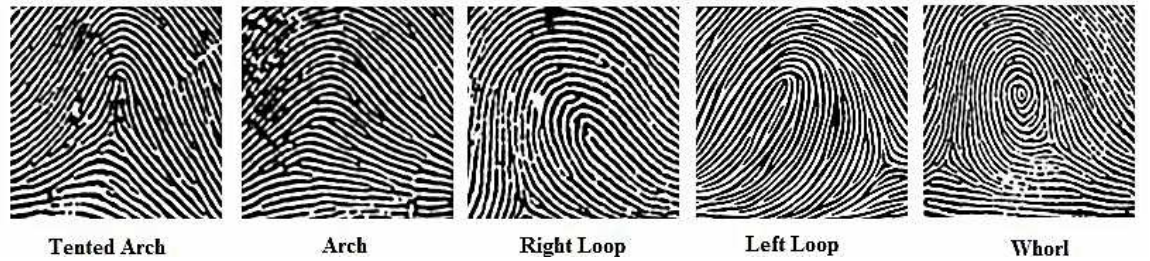

Figure 2.5: Fingerprint classes [13].

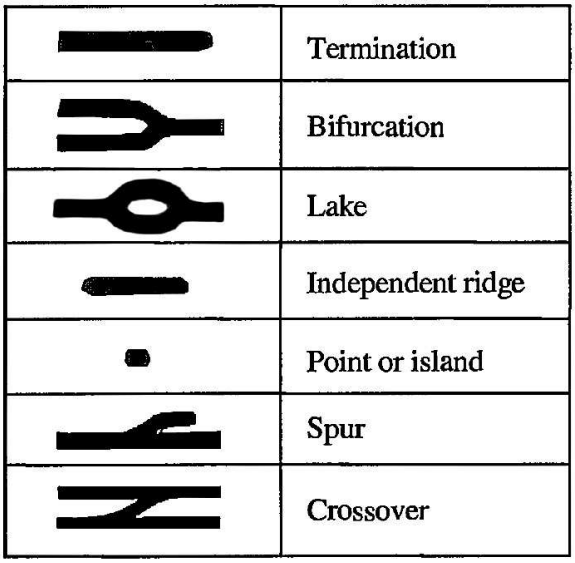

Figure 2.6: Most common fingerprint minutiae types [13].

The American National Standard Institute (ANSI) proposed a minutiae taxonomy based on four classes: terminations, bifurcations, crossovers (trifurcations), and undetermined. The FBI minutiae model takes into account only terminations and bifurcations instead. [13]

Fingerprint images can be described even further into detail by identifying *sweat pores*. This requires images to be captured at high resolution (e.g., 1,000 dpi). Matching results of methods using sweat pores only are outperforming methods using minutiae points and combination of the two techniques results in significant improvement of matching scores [26]. However, even though pore information is highly distinctive, very few automatic recognition systems use them because of high demands on image quality. [13, 11]

2.3 Fingerprint acquisition technology

From historical point of view, the only fingerprint acquisition technology available was so-called ink technique [13]. With this method, fingerprint images are collected from subjects by pressing their ink-coloured fingers against a paper card. Then the paper cards can be converted into digital form using a scanner or camera. This is referred to as off-line fingerprint acquisition or sensing.

Modern approaches of fingerprint acquisition prefer to use more sophisticated methods

of capturing fingerprint images by directly sensing the finger surface with an electronic fingerprint scanner. The most important part of a fingerprint scanner is the sensor, which is the component actually creating the fingerprint image. Almost all the existing sensors belong to one of the three categories [13]: optical, solid-state, and ultrasound, falling into the on-line (also called live-scan) sensing category.

Each technology is described in the following subsections using information acquired mainly from Jain's Handbook of Fingerprint Recognition [13] and paper by X. Xia and L. O'Gorman [24].

2.3.1 Optical sensors

One of the longest and most-commonly used technique of live-scan fingerprint acquisition is the *Frustrated Total Internal Reflection (FTIR)* technique (figure 2.7a). While the finger touches the top of glass prism, the left side is illuminated through a diffused light which is reflected by valleys and absorbed by ridges. The light exits the prism on the right side and is focused to a CCD (charge-coupled device) or CMOS (complementary metal–oxide–semiconductor) sensor.

As the technique requires a 3D surface to scan, it cannot be tricked by presenting a photograph of a fingerprint. Despite generally better image quality, devices based on FTIR technology cannot be miniaturised as well as other optical techniques can. However, one way of improving the final size of the device at the cost of lower image quality is to use a modified *FTIR technology with sheet prism* instead of a single large prism (figure 2.7b).

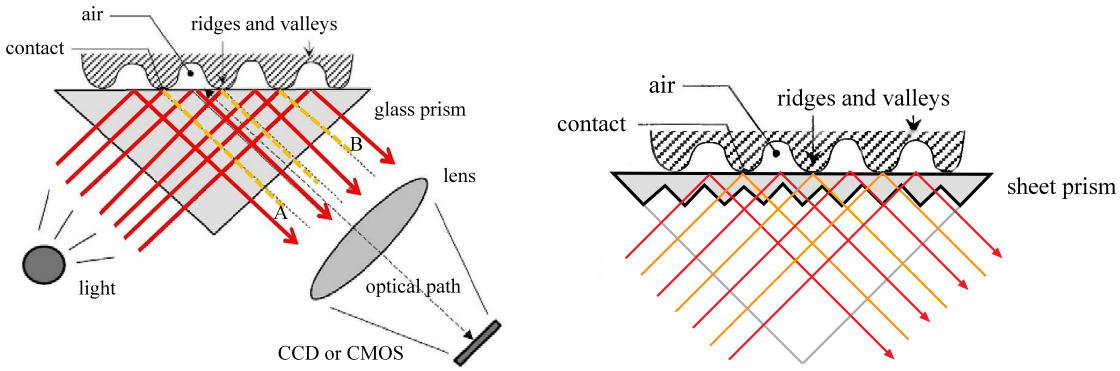

(a) FTIR (b) FTIR with sheet prism

Figure 2.7: Two FTIR-based fingerprint acquisition techniques [13].

Some of the newer optical-based sensors use *optical fibres*, allowing to further reduce the size of the scanning device (figure 2.8a). During the sensing, the finger is in a direct contact with the upper side of the fiber-optic platen. On the other side, a CCD or CMOS sensor receives light brought by the glass-fibres. As the sensor is tightly coupled with the platen, its size has to cover the whole scanning area, and this therefore makes the production more expensive.

A different approach is taken by the *electro-optical*-based scanning devices (figure 2.8b). They consist of two layers, one of them containing a polymer that upon polarisation with proper voltage emits light. As the ridges touch the layer and valleys do not, the emitted light is different. This light is then captured by the second layer which consists of photodiode array and is converted into digital image of the fingerprint.

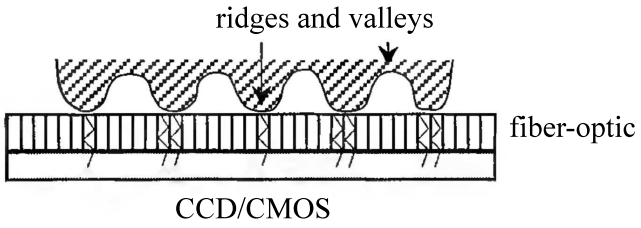

(a) Optical fibres

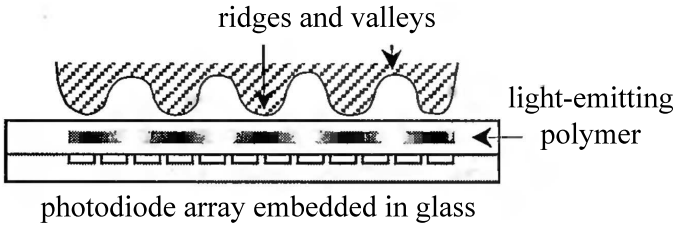

(b) Electro-optical

Figure 2.8: Optical fibres and electro-optical fingerprint sensing methods [13].

Last described method of fingerprint acquisition based on optical sensors is *direct reading*. It uses a high-quality camera to directly capture the image of a fingerprint. The finger does not get in physical contact with any surface and therefore overcomes the need to clean the scanning area surface. Other advantages over traditional methods of fingerprint sensing by pressing a finger against a hard surface are elimination of partial or degraded images. Degradation can be caused by improper finger placement, skin deformation, slippage or smearing. [6, 23]

However, capturing a well-focused and high-contrast image is not easy to do. Another challenging part of the acquisition process is the unwrapping of 3D touch-less fingerprints into 2D such that the resulting 2D fingerprints are compatible with legacy rolled fingerprints. [6]

Examples of fingerprint acquisition devices using this kind of sensor are devices made by TBS[1].

2.3.2 Solid-state sensors

Solid-state sensors were designed to overcome the cost and size issues of optical sensors. The silicon-based sensors consist of an array of pixels, each working as a stand-alone sensor itself. Therefore, there is no need for CCD or CMOS image sensors. Four main technologies are used in order to convert the captured information into digital image. They are capacitive, thermal, electric field, and piezoelectric.

The most-common used method for fingerprint sensing based on solid-state sensor is the *capacitive* method (figure 2.9). The sensor consists of a two-dimensional array of micro-capacitor plates on a chip. Upon placing the finger on the chip, small electrical charges are created between the finger and each of the silicon plates. Depending on the distance of the fingerprint surface and the plates, the magnitude of electrical charges differs. Based on them, the fingerprint image is then created.

[1] http://www.tbs-biometrics.com/

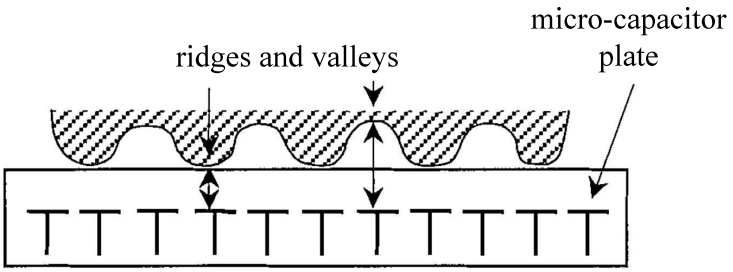

Figure 2.9: Capacitive fingerprint sensing method [13].

Another type of fingerprint capturing device uses *thermal* solid-state sensor. It is made of pyro-electric material generating current based on temperature differentials. Because ridges are in direct contact with the sensor surface, a different temperature is produced by them than the temperature produced by valleys which are further away. The sensor's surface is usually heated to increase the difference between temperatures of the finger and the sensor. The fingerprint image is produced upon contact being made. However, it soon disappears because of reaching temperature equilibrium. Therefore, it is ideal to use a sweeping method to acquire the fingerprint image.

An *electric field* sensors consist of a drive ring generating a sinusoidal signal and a matrix of active antennas capturing a small amplitude signal modulated by the derma structure. It is required that the finger stays in contact with both the sensor and the drive ring during the process of sensing.

The last representative of fingerprint sensing devices using solid-state sensors is *piezo-electric*. The idea of this kind of devices is to use pressure-sensitive sensors that generate electrical signal when mechanical pressure is applied to them. The sensor surface consists of a dielectric material that produces a small amount of current depending on the pressure applied to it. Due to the different distance of ridges and valleys, the pressure created by them is different too, thus they generate a different amount of current.

2.3.3 Ultrasound sensors

Ultrasound sensors are based on the echography technology (figure 2.10). An acoustic signal is being sent towards the fingerprint and its echo is captured. The echo signal is used to compute the fingerprint structure.

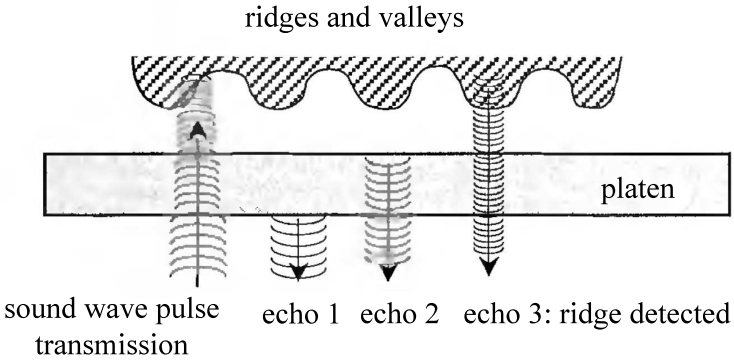

Figure 2.10: Ultrasound fingerprint sensing method [13].

The sensor is made of two main components: the transmitter and receiver. The transmitter generates short acoustic pulses and the receiver detects responses returning from the fingerprint surface. This technology allows high-quality images capturing and is resilient to dirt and oil that might visually spoil the fingerprint image.

2.4 Fingerprint recognition process

A captured fingerprint image must be processed before it can be stored or looked up in a database. Although there are methods directly comparing fingerprint images using correlation, a grey-scale fingerprint image is known to be a highly unstable representation. Most of the fingerprint-processing algorithms require image features to be identified and extracted before they are processed further.

The methods described in the following paragraphs have been adopted from biometrics-related literature [9, 19, 13].

2.4.1 Fingerprint image processing and feature extraction

The quality of fingerprint images usually differs in practice as they belong to a group of images with generally high ration of clutter. Clutter is defined as every element of the image which does not relate to the papillary lines. Fingerprint image processing algorithms aim to enhance the image quality by applying various filtering techniques in order to extract minutiae more accurately.

The first step in fingerprint image processing is *local ridge orientation estimation*. The fingerprint image is divided into smaller blocks and for each block a local ridge orientation is estimated. The fingerprint orientation image is a matrix $\mathbf{D}$ (see figure 2.11), whose elements encode the local orientation of the fingerprint ridges. Each element θ_{ij}, corresponding to the block $[i, j]$ of the square grid over the pixel $[x_i, y_j]$ denotes the average orientation of the fingerprint ridges in the neighbourhood of the pixel. Also an additional value r_{ij}, associated with every element, evaluates the consistency of each orientation estimation.

The easiest way for extracting the local ridge orientation uses fingerprint image gradients computation. The gradient $\nabla(x_i, y_j)$ at pixel $[x_i, y_j]$ is a two-dimensional vector $[\nabla_x(x_i, y_j), \nabla_y(x_i, y_j)]$, where ∇_x and ∇_y are the derivative of pixel $[x_i, y_j]$ in the image with respect to the x and y directions. Therefore, the direction θ_{ij} of image block centred at $[x_i, y_j]$ is orthogonal to the gradient phase angle at $[x_i, y_j]$.

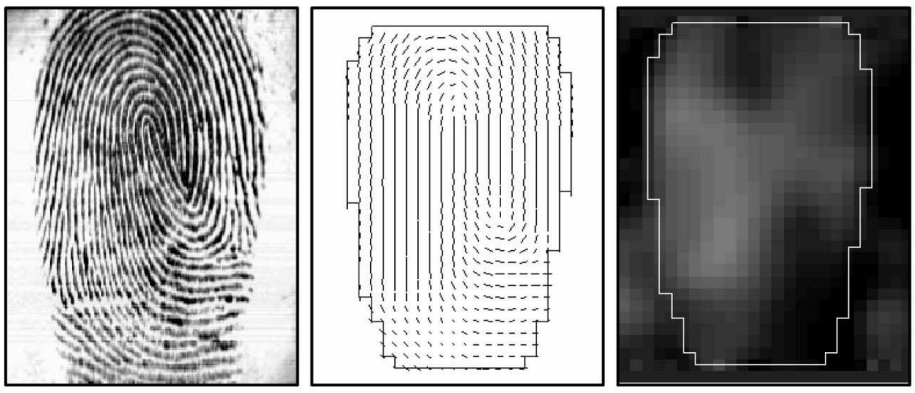

Figure 2.11: Local ridge frequency estimation [2].

The fingerprint image processing continues with *local ridge frequency estimation* denoted as f_{xy} at point $[x, y]$. The local ridge frequency represents the inverse of the number of ridges per unit length along the segment of the fingerprint image centred at $[x, y]$ and orthogonal to previously computed local ridge orientation θ_{xy}. A matrix of computed frequency for each block of the image is then called a frequency image $\mathbf{F}$ (figure 2.11).

In order to make further steps of fingerprint image processing more efficient, image enhancing techniques have to be used. In practice, several different methods of image enhancement are commonly applied. The simplest one is image thresholding technique, however in low-quality images, it is not able to produce good results. A more efficient approach to discriminating fingerprint from the background is based on the idea of isolating the fingerprint area according to local histograms of ridge orientations. Other methods such as using the average magnitude of the gradient in each image block or enhancing image using Gabor filters are used as well.

Finally, before minutiae detection from the fingerprint image is done, ridge thinning technique is often applied in order to reduce the width of the ridges to one pixel.

2.4.2 Minutiae detection

Once a binary skeleton of fingerprint has been obtained, the image is scanned through in order to detect pixels corresponding to different minutiae by computing the so-called crossing number (see equation 2.1).

The crossing number $cn(p)$ of a pixel p is defined as half the sum of the differences between pairs of adjacent pixels in the 8-neighbourhood of p:

$$cn(p) = \frac{1}{2} \sum_{i=1..8} |val(p_{i \bmod 8}) - val(p_{i-1})|, \tag{2.1}$$

where $p_{0..7}$ are the pixels defining the 8-neighbourhood of p and $val(p) \in \{0, 1\}$ is the pixel value. With crossing number defined, it is simple to note (see figure 2.12) that a pixel p with $val(p) = 1$ and corresponding number value:

- is an intermediate ridge point if $cn(p) = 2$,
- defines a termination minutia when $cn(p) = 1$, and
- defines a more complex minutia (bifurcation, crossover, etc.) in case $cn(p) \geq 2$.

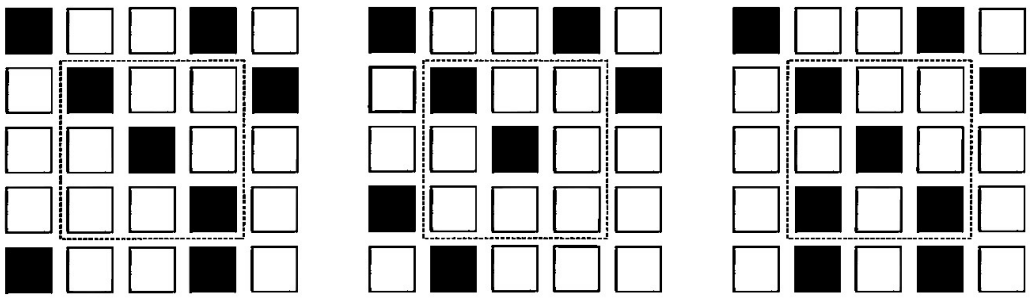

Figure 2.12: An intra-ridge pixel; termination minutia; bifurcation minutia [13].

A post-processing stage in minutiae detection step is often useful in order to filter out minutiae detected in corrupted regions of image or wrongly detected minutiae brought in by some of the image enhancement techniques.

Simple structural rules might be used in order to remove false minutiae structures. The algorithm is based on predefined rules and as input, it requires minutiae characteristics such as the length of the associated ridge(s), the minutia angle, and the number of facing minutiae in the neighbourhood. As shown in figure 2.13, the algorithm connects facing endpoints (a, b), removes bifurcations facing with endpoints (c) or with other bifurcations (d), and removes spurs (e), bridges (f), triangles (g), and ladder structures (h).

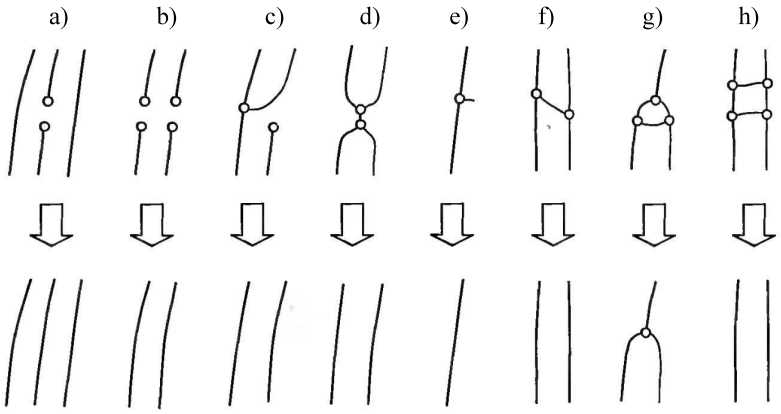

Figure 2.13: The false minutia structures correction rules [13].

2.5 Synthetic fingerprint

With the ever-growing progress of fingerprint recognition systems adoption in many different areas, methodical and accurate performance evaluations of fingerprint recognition algorithms are needed. The evaluation is usually based on their recognition accuracy on test data. The evaluation process consists of three main steps [25]:

1. fingerprint images acquisition,
2. features extraction and matching in order to generate match scores,
3. match scores analysis in order to compute error rates.

Due to very small error rates to be estimated, a reliable evaluation method requires large databases of fingerprints. However, collection of a large database of fingerprints is [2]:

1. expensive in terms of money,
2. time-consuming,
3. problematic due to privacy legislation that applies to biometric features.

Synthetic fingerprint database has been used for example at a performance evaluation event *FVC2006 [3] (Fingerprint Verification Competition 2006)* along with three other databases containing real fingerprints. [4]

In order to overcome the difficult and time-consuming process of fingerprint collection, synthetic fingerprint generators can be used to produce large databases at very low cost in terms of money and time. Several methods have been presented and published that produce authentic images of fingerprints. Their detailed description follows.

2.5.1 SFinGe

One of the first approaches to realistic synthetic fingerprint image generation has been introduced by R. Cappelli from the University of Bologna in 2004 [2]. The synthetic fingerprints generated emulate real images acquired with on-line sensors such as capacitive or optical ones.

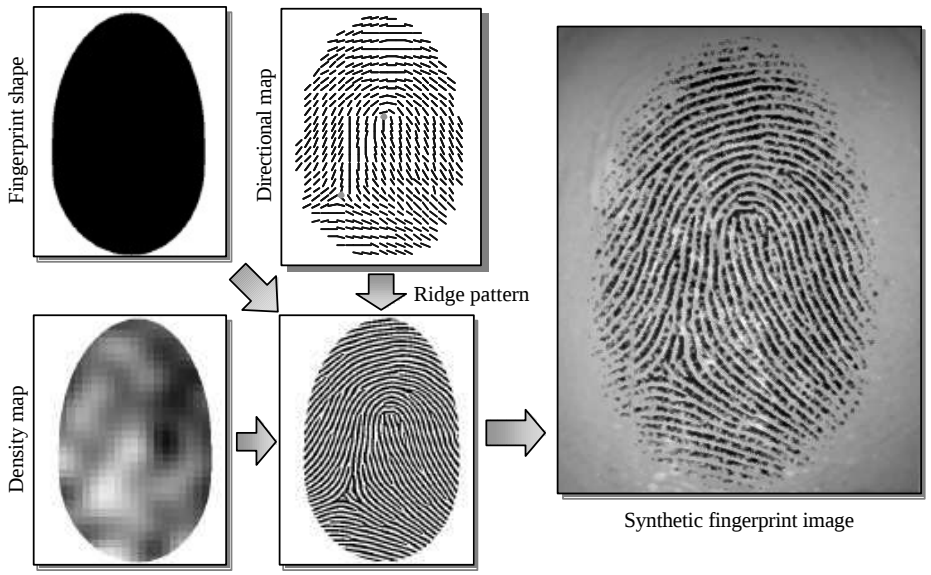

Figure 2.14: Basic steps of SFinGe method [2].

The basic steps to create a synthetic fingerprint image are: generate a fingerprint shape, a directional map and density map separately and combine the three features afterwards. The process of fingerprint generation process can be seen in figure 2.14. SFinGe method uses a master-fingerprint in order to derive several synthetic images of the same fingerprint.

The process of generating the master fingerprint (steps 1–4) and fingerprint impression (steps 5–10) consists of the following steps:

1. fingerprint shape generation;
2. directional map generation;
3. density map generation;
4. ridge pattern generation;
5. contact region selection;
6. image erosion or dilation;
7. fingerprint distortion;
8. noising and rendering;
9. global translation and rotation;
10. background generation.

Step 1 defines the final shape of generated fingerprint; step 2 utilises a mathematical ridge-flow model to generate a consistent directional map considering the fingerprint class and position of singularities; step 3 creates a density map based on real fingerprint images; in step 4 the ridge-line pattern and minutiae are created using a space-variant linear filtering.

In order to create different impressions of the same master-fingerprint the following steps are made. Step 5 simulates different placement of the finger over the acquisition sensor by

translating the ridge pattern randomly without modifying the global shape and position. In step 6, the erosion operator is applied to simulate dry skin and oppositely dilatation is used to make the skin wetter. Step 7 generates realistic impressions by using a skin distortion model, while step 8 adds some noise to the image simulating pores in between the ridges and different contact with the sensor. Finally, step 9 makes fingerprint images randomly rotated and translated and step 10 generates realistic background for the fingerprint image based on selected sensor technology.

Figure 2.15: Example fingerprints generated by SFinGe method.

SFinGe method is a mature synthetic fingerprint algorithm with a large variety of settings that can be modified. It produces high-quality images of realistic fingerprints (an example of generated fingerprint image can be seen in figure 2.15). Authors provide two versions of the software tool, a free version limited to generating one fingerprint at a time, and a full version capable of generating whole databases of hundreds of fingerprints.

2.5.2 Radek Chaloupka's method

Another way to generating synthetic fingerprint images has been published by Radek Chaloupka in his master thesis in 2007 [5].

In his work, Chaloupka chooses a modified approach from the SFinGe method. While SFinGe isn't supplied with minutiae in advance, a complete fingerprint image is generated based only on the selected shape and fingerprint class. Chaloupka's method works with minutiae type and position defined before the generation of fingerprint image begins.

The steps of fingerprint generation are as follows [5]:

1. directional map generation;
2. density map generation;
3. ridge pattern generation;
4. fingerprint shape generation.

Step 1 is the most important one in the whole generation process as it defines the final fingerprint ridges appearance. Directional map generation is based on already known positions and types of minutiae defined. For every pixel in image, the direction based on the closest minutia is computed. In step 2, random density map is generated. Ridge pattern generation in step 3 uses the same set of Gabor linear filters as SFinGe method does. The only difference is that here, the filtering cannot be applied to the whole image

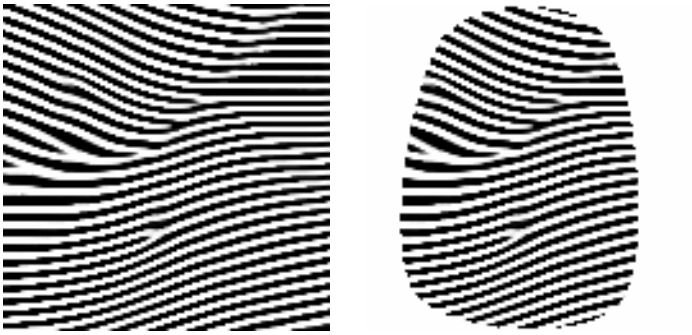

Figure 2.16: Fingerprints generated by Chaloupka's method (shape generation) [5].

as the already existing minutiae must be kept intact. As the last step, the final fingerprint shape is selected by applying mask on the generated image.

Fingerprint image generation method proposed by Radek Chaloupka is largely based on the SFinGe method. Even though the images generated by this method might at first glance look realistic, after examining them more in detail, one can notice that the fingerprints do not respect existing fingerprint classes (see figure 2.16). Therefore, they are not suitable for most use cases in comparison with images generated by SFinGe method.

2.5.3 Statistical feature models based method

The most recent approach to generate synthetic fingerprint images is by Zhao et al., published in 2012 [25]. It's goal is to improve SFinGe method by retaining specified features (orientation field, minutiae) chosen in advance. The method is based on sampling fingerprint features from statistical models established for each of the types of fingerprint (i.e. arch, tented arch, left loop, right loop, and whorl).

The fingerprint image synthesis algorithm consists of the four following steps [25]:

1. sampling fingerprint features from statistical models;
2. master fingerprint generation;
3. fingerprint impressions generations;
4. rendering fingerprint images.

In step 1, the method sequentially samples the fingerprint features from statistical models based on a given fingerprint type. First, singular points are sampled, followed by orientation field and minutiae. In step 2, the master fingerprint is reconstructed from a set of sampled features using the AM-FM based method. This results in a relatively small number of missing minutiae. Afterwards, fingerprint impressions are generated in step 3. This is done by distorting the master fingerprint by applying non-linear plastic distortion followed by global rigid transformation. The final step 4 renders the fingerprint image and simulates the finger dryness and adds noise.

Zhao's method of fingerprint image generation aims at improving the SFinGe method by distributing the generated minutiae on the fingerprint image more evenly based on a selected statistical model (see comparison of fingerprints generated by SFinGe and method proposed by Zhao in figure 2.17).

Figure 2.17: SFinGe fingerprint; and Stat. feature models based method fingerprint [25].

2.6 Disease-affected fingerprints

Although it is well-known that fingerprints do not change with time, images of the same captured finger can become quite different over a period of time due to many factors. These include injuries and bruises, peeling of the skin on the finger, current dryness of the skin, and also developing a skin disease affecting person's skin on fingers. [14]

Skin diseases represent an important factor of fingerprint acquirement process. It is however often left out of consideration. Therefore, patients with fingerprint-affecting diseases are often unable to use fingerprint scanners in order to authenticate into a given system.

The fact that this subject is ignored is supported by missing research in this area of fingerprint biometrics. Only two recent academic works conducted by Drahansky et al. [8] and Lee et al. [17] explore the effects of skin diseases on the fingerprint acquisition process. The work of Lee et al. concentrates on patients with hand dermatitis while the work of Drahansky et al. considers several different diseases and at the same time presents a way of enhancing the disease-affected fingerprint image to improve the success rate of enrolment and matching.

Even though it is impossible to estimate the total number of people with skin diseases, about 20–25% of patients in general medical practice are reported to have some sort of skin-related problems [8]. It is important to note that patients after successful recovery from the disease can use the fingerprint authentication again in the case the disease had not attacked and destroyed the structure of papillary lines in the two top layers of the skin: epidermis and dermis.

A list of several selected most common diseases divided into three categories by their effects on skin follows. Information in this section is based on research published by Drahansky et al. [8] and clinical Dermatology books [15, 10].

2.6.1 Diseases causing histopathological changes of epidermis and dermis

The following diseases might cause problems for most of sensor types as the colour and structure of epidermis and dermis are affected.

(a) Hand eczema (b) Fingerprint eczema (c) Pompholyx

Figure 2.18: Skin diseases (hand eczema, fingerprint eczema, and pompholyx) [8, 15].

Hand eczema [10] is an inflammatory non-infectious long-lasting relapsing disease. It is one of the most common skin diseases with prevalence reaching approximately 5.4%. The most common type of eczema is irritant contact dermatitis, atopic eczema, and allergic contact dermatitis. Acute form is characterized by presence of erythema, swelling, blisters, and crusts (figure 2.18a).

Fingertip eczema [10] is very dry chronic form of eczema of the palmar surface of the fingertip affecting one or several fingers. Initially the skin may be moist and then become dry, cracked, and scaly. The skin peels from the fingertips distally, exposing a very dry, red, cracked, tender, or painful surface without skin lines (figure 2.18b).

Pompholyx (dishidrosis) [15] is one of the most common skin disorders. It is not related to blockage of sweat ducts, although palmoplantar hyperhidrosis is common in these patients. Itching precedes the appearance of tiny water-filled vesicles on the palms and sides of the fingers which are relatively deep seated. The skin may be red and wet (figure 2.18c).

Pyoderma [8] is a sign of bacterial infection of the skin. It is caused by *Staphylococcus aureus* or *Streptococcus pyogenes*. Blistering distal dactylitis is specific type of pyoderma and is characterized by tense superficial blisters occurring (figure 2.19a).

Herpes simplex virus [8] infection may uncommonly occur on the fingers. Lesions begin with tenderness and erythema and deep-seated blisters develop until 48 hours after symptoms occur. In the host with systemic immune-compromise, Herpes simplex may cause chronic ulcerations (figure 2.19b)

Leprosy [15] is a chronic granulomatous disease caused by *M. leprae*, usually acquired during childhood/young adulthood. It is disease of the developing world. Lepromatous type can lead to loss of tissue of fingertip (figure 2.19c).

(a) Pyoderma (b) Herpes simplex (c) Leprosy

Figure 2.19: Skin diseases (pyoderma, herpes simplex, and leprosy) [8, 15].

2.6.2 Diseases causing skin discolouration

The following diseases often make it difficult to capture fingerprint using optical sensors.

Hand, foot, and mouth disease (HFMD) [15] is a contagious infection occurring primarily in children and characterized by a vesicular palmoplantar eruption. The skin lesions begin as red macules that rapidly become pale, white, oval vesicles with red areola (figure 2.20a).

Scarlet fever (scarlatina) [8] is contagious disease caused by *β-hemolytic Streptococcus* that produces an erythrogenic toxin. In the final stages of the disease, large sheets of epidermis may be shed from the palms in glove-like cast, exposing new tender and red epidermis beneath (figure 2.20b).

Secondary syphilis [8, 15] starts at about the 9^{th} week of infection and is characterized by lesions, which may assume a variety of shapes, including round, elliptic, or annular. These lesions are called syphilids. Semirigid small lesions of red-brown colour with scaling may be observed on palms, soles, and fingers (figure 2.20c).

(a) HFMD (b) Scarlet fever (c) Secondary syphilis

Figure 2.20: Skin diseases (HFMD, scarlet fever, and secondary syphilis) [8, 15].

2.6.3 Diseases causing histopathological changes in junction of epidermis and dermis

The following diseases are mainly focused on ultrasonic sensors, which detect the base of papillary lines on the border of epidermis and dermis. Some of them can be also set to the first group.

(a) Warts (b) Psoriasis

Figure 2.21: Skin diseases (warts, psoriasis) [15].

Warts (*verruca vulgaris*) [8] are benign epidermal neoplasms that are caused by human papilloma viruses (HPVs). Warts commonly appear at sites of trauma, on fingers of both hands. HPVs induce hyperplasia and hyperkeratosis (figure 2.21a).

Psoriasis [8] is characterized by scaly papules and plaques. The disease is transmitted genetically and is lifelong. It is characterized by chronic, recurrent exacerbations and remissions. Psoriasis of the palms and fingertips is characterized by red plaques with thick brown scale. The lamellar scales are more adherent and only their removal will reveal the reddish inflammatory base (figure 2.21b).

Chapter 3

Analysis and design of methods simulating disease-affected fingerprint

The following chapter contains analysis of existing fingerprint images damaged by selected diseases and the method design of simulating similarly modified skin disease-affected fingerprint images from synthetic fingerprints.

The thesis goals are outlined and elaborated in section 3.1. Section 3.2 describes the STRaDe database of fingerprints acquired from patients with various skin diseases. In the next two sections, section 3.3 and 3.4, selected skin diseases are described in detail, existing disease-affected fingerprint images are analysed, and methods of simulating similar disease marks to a synthetic fingerprints are proposed.

3.1 Thesis goals elaboration

The task assigned for this thesis has been to select up to two most common fingerprint-affecting diseases from the available subset of STRaDe database and design an algorithm modifying a synthetic fingerprint image in a way similar to the way a real disease would. The implemented algorithm should then be used to generate a set of at least a hundred fingerprints affected by selected diseases. With the generated datasets, experiments should be conducted to verify the influence of fingerprint-affecting diseases on the fingerprint recognition process.

The STRaDe database contains fingerprint images acquired via several different devices using different sensing technology (see the following section 3.2 for more details). As the appearance of disease marks can differ due to different technology of acquisition used, the work will concentrate only on fingerprints acquired using the optical technology (including digitalized fingerprint images acquired using the ink-method).

Because diseases can affect fingerprint in various extent, it has been decided to exclude from further examination those fingerprint images that are heavily damaged by the disease. The excluded group consists of fingerprints missing all ridge structure or structure visible only on a small area (less than 25% of the fingerprint).

The methods designed shall respect the outlined constraints. The synthetic fingerprint generator is to be set to produce undamaged synthetic fingerprint images simulating the optical technology of sensing. The final damaged fingerprint images shall preserve the ridge structure in a way that it is still visible at least on 25% of the fingerprint area.

3.2 STRaDe fingerprint database

A subset of a fingerprint database has been acquired from the STRaDe research group[1] at Brno University of Technology. The whole database consists of thousands of fingerprint images (the available subset is made up of 750 images) acquired directly from patients with various skin diseases. The sensing methods and devices used to capture the fingerprint images include ink technique, Sagem MSO 300[2], TBS 3D Enroll[3], UPEK Eikon II, UPEK EikonTouch 500[4], and Dino-Lite microscope[5].

The range of diseases the database contains include acrodermatitis (figure 3.1a), atopic dermatitis also known as atopic eczema (figure 3.1b), warts (figure 3.1c), dyshidrosis (figure 3.1d), hyperkeratotic eczema (figure 3.1e), lupus (figure 3.1f), and several other, less common illnesses.

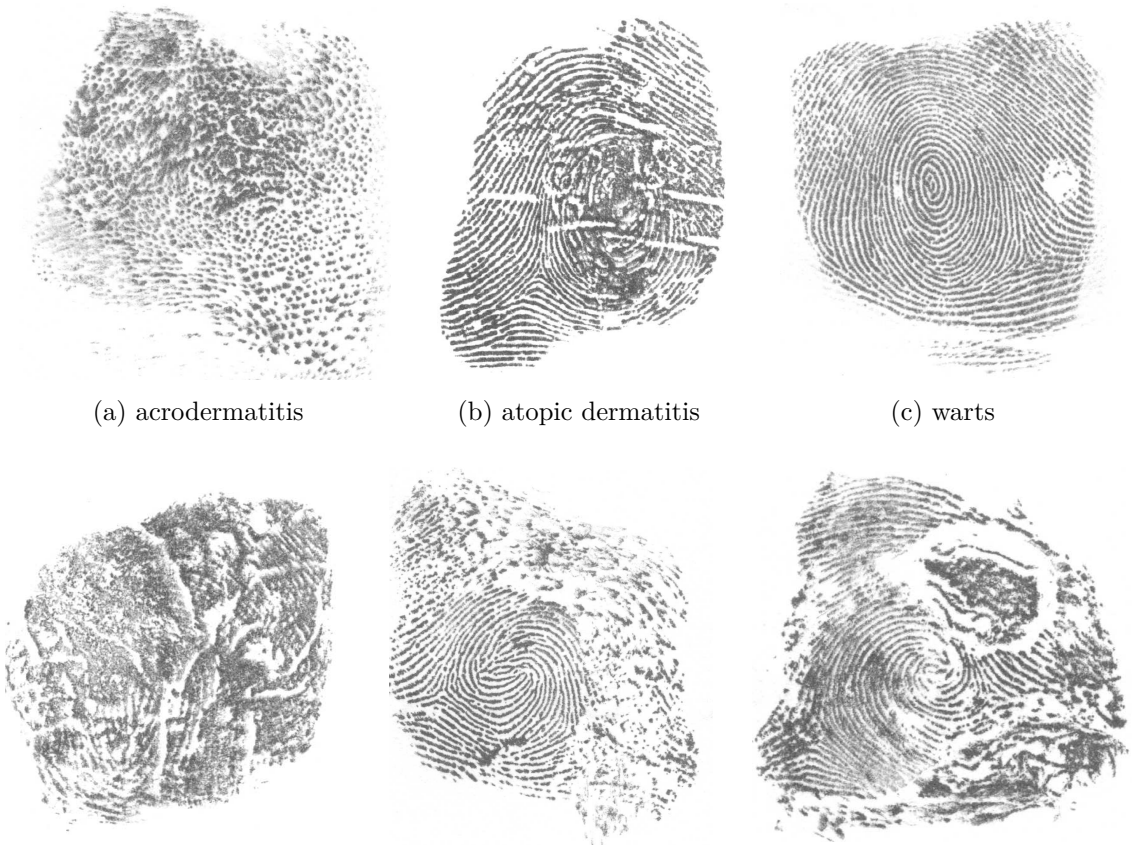

(a) acrodermatitis (b) atopic dermatitis (c) warts

(d) dyshidrosis (e) hyperkeratotic eczema (f) lupus

Figure 3.1: Examples of disease-affected fingerprints from STRaDe database.

For the purpose of this thesis, the two most-common fingerprint-affecting skin diseases have been chosen: *warts* and *atopic eczema*. The two diseases are analysed in more detail in the following sections of this chapter.

[1] http://strade-fs.fit.vutbr.cz/cms/en/
[2] http://www.morpho.com/en/biometric-terminals/desktop-devices/fingerprint-devices/
[3] http://www.tbs-biometrics.com/en/hardware/
[4] http://www.crossmatch.com/eikon-usb-readers/
[5] http://www.dino-lite.com/

3.3 Warts

The first skin disease chosen for simulation are warts, specifically common warts (*verruca vulgaris*). In the following sections, the disease is described in detail (adapted mainly from [15]), analysis of selected representative set of wart-affected fingerprints is conducted and a method of simulating similarly-looking fingerprint images affected by warts is proposed.

3.3.1 Warts: disease description

Warts are caused by human papillomaviruse (HPV) which belongs to a group of papovaviruses. There is more than a hundred of types of HPV and gene sequences of HPVs throughout the world are similar. Most of them cause specific types of warts and favour certain anatomic locations, such as plantar warts, common warts, genital warts, and so on.

HPV infection is very common amongst the world population, as most people will experience it during their lifetime. HPVs have coexisted with humans for many millennia, and humans are also their primary host. HPVs have been successful pathogens of human because they evade their immune response.

Common warts are the most-spread variant of warts (affecting approximately 10% of the population [21]) and usually cause frustration on the part of the patient. Social activities can be affected, lesions can be uncomfortable or bleed, and treatment is often painful and frustratingly ineffective [7]. Frequent immersion of hands in water is a risk factor for common warts. People working with raw meat have a high incidence of common warts of the hands.

Common warts are usually located on the hands, favouring the fingers and palms (see figure 3.2). Periungual warts are more common in nail biters. Fissuring may lead to bleeding and tenderness. Lesions range in size from pinpoint to more than 1 cm, most averaging about 5 mm. They grow in size for weeks to months and usually present as elevated, rounded papules with a rough, grayish surface. In some instances, a single wart (mother wart) appears and grows slowly for a long time, and then suddenly many new warts erupt. On the surface of the wart, tiny black dots may be visible, representing thrombosed, dilated capillaries. Warts do not have fingerprint folds, as opposed to calluses, in which these lines are accentuated.

(a) (b)

Figure 3.2: Common warts on hands and fingers [15].

Treatments for common warts involve two basic approaches: destruction of the wart and induction of local immune reactions. Destructive methods are most commonly used as initial therapy by most practitioners. Cryotherapy is a reasonable first-line therapy for most common warts. The wart should be frozen adequately to produce a blister after one or two days. An alternative method of treatment gaining on popularity is a pulsed dye laser treatment which is both effective and safe for the patient [21].

3.3.2 Warts-affected fingerprint analysis

The STRaDe fingerprint database contains fingerprint images acquired by various methods and sensors. To study possible differences between images acquired by different sensors, three fingerprints of the same finger affected by warts have been chosen (see figure 3.3). Figure 3.3a has been acquired using the ink technique, Sagem MSO 300 sensor has been used to capture figure 3.3b, and figure 3.3c has been acquired by UPEK Eikon II sensor.

On figures 3.3a and 3.3b, it can be seen that the wart is located just on top of the whorl. It is a white oval with irregular border. Inside the oval, there are black dots. The ridge structure is completely disrupted by the wart. However, the ridge flow continues normally around the border of the wart. Image 3.3c acquired by UPEK sensor cuts the wart out of the image completely.

(a) ink technique (b) Sagem MSO 300 (c) UPEK Eikon II

Figure 3.3: Same fingerprint affected by warts acquired by different sensors.

Let us now compare three different fingerprint images affected by warts (figure 3.4) that have been captured using a single sensor, in this case Sagem MSO 300.

The first figure 3.4a shows a fingerprint with a clean ridge structure except for the part where the wart is located. The wart is located near the right border of the image and on the image it is represented by a white circle-shaped object with several black dots irregularly spread over its surface. In the upper part of the fingerprint image, another small oval-shaped structure can be seen. It could be a small wart that has spread from the larger one. When the wart is relatively small, usually it contains little or no black dots at all.

In the second figure 3.4b, a single large wart is located near the whorl. Black dots on top of it represent the hard and scaly skin of the wart. The wart is irregularly shaped and its border is well-defined. The ridge structure around the wart is mildly deformed and the ridges are compressed. However, except for the close surroundings of the wart, the ridge structure of the fingerprint is unaffected.

The third figure 3.4c shows a fingerprint that has been affected by warts in a large area

of its surface. There are at least three large white oval-like objects with irregular borders near each other. The warts affect the ridge structure near their edges similarly as the wart described previously.

(a) (b) (c)

Figure 3.4: Different fingerprints affected by warts acquired by Sagem MSO 300.

From the available subset of STRaDe database of fingerprints, it has been found that the size of warts on fingers varies from very small ones to ones as large as half of the hypothetical radius of the fingerprint. The location of warts on fingerprint is completely random and often one wart produces other so-called satellite warts in its close surroundings.

3.3.3 Design of a method for warts-affected fingerprint generation

Based on the analysis of existing fingerprints affected with warts, design of a method for generating similar synthetic fingerprint images is proposed in this section. The algorithm consists of the following steps:

1. localise the fingerprint area on the image;
2. determine the new wart size and locate its centre point in the fingerprint;
3. draw the wart into an image buffer:
   (a) create an empty image buffer;
   (b) generate a number of small circles around the centre point of the wart;
   (c) draw the generated circles into the buffer;
   (d) draw dark dots inside the wart;
   (e) determine the final colour of each wart pixel;
   (f) blur the wart in the buffer.
4. draw the wart from the image buffer into the fingerprint image;
5. generate possible secondary warts.

In order to generate warts into the image with synthetic fingerprint, the fingerprint has to be localised in the input image first. This is done in step 1. First, an adaptive thresholding is applied in order to clearly separate the fingerprint structure from background. Then the image is blurred so that the fingerprint ridges connect and contours can be localised in the image. The contour of the largest area is then selected as the fingerprint contour (see figure 3.5). This contour then defines the border of the fingerprint.

In step 2, a centre of the new wart is localised. The point coordinates are randomly generated and are used only if they comply with the requirements (location inside of the

(a) Original fingerprint (b) Blurring applied (c) Fingerprint contour

Figure 3.5: Fingerprint area localisation (step 1).

fingerprint, minimal distance from the fingerprint border). Also in this step, the size of the generated wart is randomly determined within boundaries set.

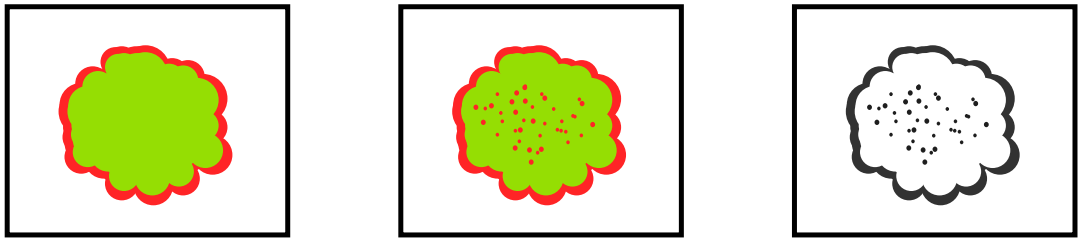

(a) Wart drawn in distinctive colours (b) Wart with dots added (c) Wart drawn in final colours

Figure 3.6: Wart drawing (into buffer).

Each new wart is first drawn into its own image buffer as not to interfere with the rest of the fingerprint. This is done in step 3 (see figure 3.6). First, an empty buffer of a size large enough for the new wart to fit in is created (step 3a). In the following step 3b, a number of small circles of varying radius is generated with their centres being distributed with exponentially large distance from the wart centre point. In the next step 3c, the previously generated circles are drawn into the buffer in distinctive colour (e.g. red or green) with their border drawn in a different distinctive colour (figure 3.6a). The final drawing step is step 3d in which the dots with randomly generated coordinates are drawn onto the warts surface. The dots are drawn with the same colour as the border of the small circles in the previous step (figure 3.6b).

With the wart shape drawn in the buffer, the algorithm proceeds with step 3e where the final colour of each pixel of the wart is determined (figure 3.6c). Depending on if the pixel is drawn by colour for border or the colour of the inside of the wart, the colour of the neighbouring pixels in the original fingerprint image is acquired (in this case dark pixels for border and light ones for the inside of the wart). The final pixel colour is then determined by one of the two following methods. First method picks random neighbouring pixel and copies its colour. The second method computes the mean colour of all the neighbouring

(a) Wart buffer drawn into the original image

(b) Secondary warts

Figure 3.7: Wart drawing (steps 4 and 5).

pixels and then the mean colour is computed and applied to the pixel. Afterwards the buffer image is blurred slightly in step 3f in order to better fit into the original fingerprint image.

Finally, in step 4 the buffer is drawn into the original fingerprint image taking in consideration the transparency of the pixels in the buffer and blending them into the original image appropriately (figure 3.7a).

Eventually, secondary warts are drawn into the fingerprint if required in step 5 following the same steps of the algorithm as for the main wart (figure 3.7b). The only difference is an added requirement not to overdraw already existing warts in the image.

3.4 Atopic dermatitis

The second of the two chosen skin diseases is atopic dermatitis (also known as atopic eczema). In the following sections, the disease is described in detail with focus on hand eczema (adapted from [15]), analysis of selected representative set of atopic dermatitis-affected fingerprints is conducted and a method of simulating fingerprint images affected by this disease is described.

3.4.1 Atopic dermatitis: disease description

Atopic dermatitis (AD) [15] is a chronic, inflammatory skin disease that is characterized by pruritus and a chronic course of exacerbations and remissions. The prevalence of AD increased dramatically in the last half of the twentieth century, becoming a severe health problem in many countries. Rates of AD are around 15–20% worldwide with up to 20% of children affected by the disease [20].

The skin, in general, is dry and somewhat erythematous. Lichenification and prurigo-like papules are common. Papular lesions tend to be dry, slightly elevated, and flat-topped. They are nearly always excoriated and often coalesce to form plaques.

Figure 3.8: Hand eczema [15].

The hands, including the wrists, are frequently involved in adults, and hand dermatitis is a common problem for adults with a history of AD. Hand eczema (figure 3.8) is the most common occupational skin condition, accounting for more than 80% of all occupational dermatitis. Women are at increased risk for the development of hand eczema. Most of this increased risk is accounted for by a spike in the rate of hand eczema in the age of 20–29 because of increased environmental exposures.

There are five different types of hand eczema [15]:

1. allergic contact dermatitis,
2. irritant hand dermatitis,
3. atopic hand eczema,
4. vesicular endogenous hand eczema,
5. hyperkeratotic endogenous hand eczema.

3.4.2 Atopic dermatitis-affected fingerprint analysis

As in the case of warts-affected fingerprints, in order to study the differences between images acquired by different sensors, three fingerprint images of the same finger have been selected (see figure 3.9). Figure 3.9a has been acquired using the ink technique, to capture figure 3.9b, Sagem MSO 300 sensor has been used, and in case of figure 3.9c, UPEK Eikon II sensor has been used.

Comparison of the three images shows no significant difference in capturing quality among them. Abnormal white lines can be seen on all three of them as well as patches of light and dark colour. Light patches are located mainly on the outer parts of the fingerprint, while dark areas are concentrated mostly in the centre of the fingerprint.

Let us now analyse four different fingerprint images affected by atopic dermatitis (see figure 3.10) that have been captured using a single sensor, Sagem MSO 300.

The first figure 3.10a shows clearly wide and long white lines running throughout the whole fingerprint. The lines are mostly horizontally oriented. The finger is dry and ridge structure is in some areas of the fingerprint image less visible than in an image of a healthy finger. On the other hand, other parts of the fingerprint show unusually dark areas with a damaged ridge structure.

(a) ink technique (b) Sagem MSO 300 (c) UPEK Eikon II

Figure 3.9: Same fingerprint affected by atopic dermatitis acquired by different sensors.

Figure 3.10b is similar in the structure of the abnormal white lines to the previously described one. The lines run predominantly in horizontal direction with their length as large as the width of the fingerprint. Other thinner and shorter white lines can be seen in both, horizontal and vertical directions. The ridge structure is clearer than on the previous fingerprint image, however the patches are present as well.

Fingerprint on figure 3.10c contains many large white-only patches with no ridge structure whatsoever. In the centre of the image, there is a wide line running from the bottom-left corner through the centre of the fingerprint to the upper-right corner of the image. Other thinner lines can be seen in the left half of the fingerprint. As the ridge structure is mostly badly damaged, this fingerprint image can hardly be used in an authentication system.

Figure 3.10d is the last fingerprint of the described set. It is similar to the first analysed fingerprint image with white lines running throughout it. In contrast with the other images, this one's lines are not as wide and run only in horizontal direction. Also, the white lines are considerably shorter. Several small white patches covering the ridge structure can be seen in the upper part of the fingerprint image.

To sum up, the two types of damage by atopic dermatitis are abnormal white lines and light and dark patches. According to Lee et al., the patches represent dystrophy of the skin and the median percentage of the surface area of dystrophy in their study was 22.80% [17].

The abnormal white lines usually run in horizontal or vertical direction and their length ranges from very short up to lines running throughout the whole fingerprint. According to the study of Lee et al., the median number of white lines per fingerprint was 12 and short horizontal lines prevailed (with occurrence in 73.0%), followed by short vertical lines (56.5%), long horizontal lines (52.5%), and long vertical lines (18.0%) [17].

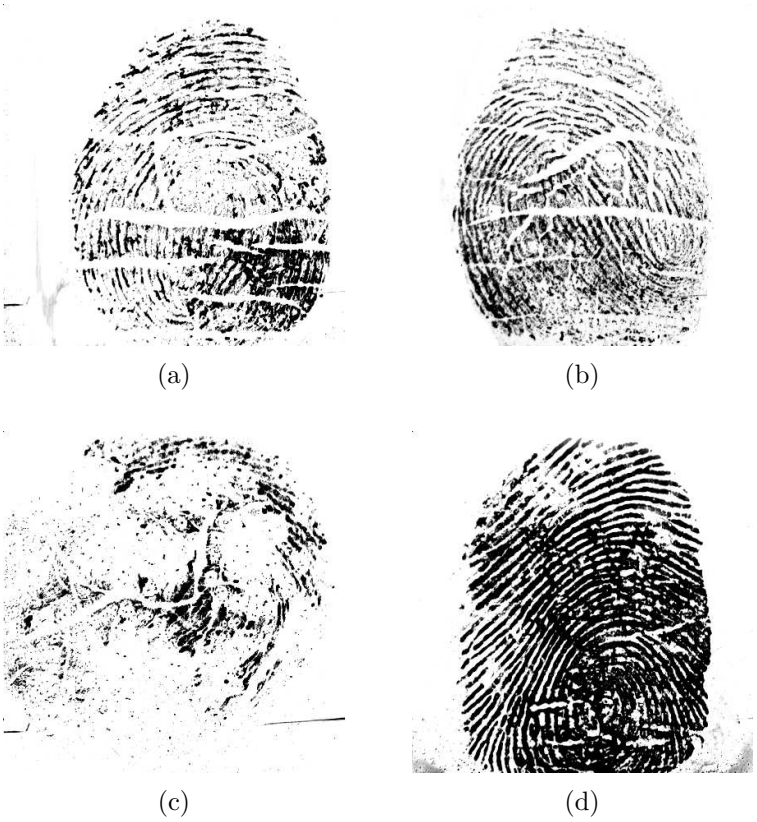

(a) (b)

(c) (d)

Figure 3.10: A set of fingerprints affected by atopic eczema acquired by Sagem MSO 300.

3.4.3 Design of a method for generation of atopic dermatitis-affected fingerprint

Based on the analysis of existing fingerprints affected with atopic eczema, design of a method for generating similarly damaged synthetic fingerprint images is proposed in this section. The algorithm consists of the following steps:

1. localise the fingerprint area on the image;
2. create an empty image buffer;
3. draw eczema patches into a buffer:
   (a) determine the centre and size of the patch;
   (b) draw the patch of determined type (light, dark).
4. determine the final colour of each pixel of the patches;
5. blur the patches in image buffer;
6. draw eczema white lines into the buffer:
   (a) determine the starting point, direction, and length of the line;
   (b) generate line points in given direction and length;
   (c) interpolate the generated line points;
   (d) draw the lines in determined thickness.
7. blur the lines in image buffer;
8. draw the buffer into the fingerprint image.

Step 1 of the algorithm is identical to the first step of the algorithm for generating warts. The result of this step is a contour of the fingerprint on the input image. Knowing precisely where on the image is the fingerprint located is necessary in order to draw onto the fingerprint area only and not outside of it.

In step 2, a new image buffer is created. The size of the buffer is the same as the size of the input image. The patches and white lines shall be drawn into the buffer separately as not to interfere with the original image.

First the light and dark patches are drawn into the buffer in step 3. The number of patches is generated randomly within set boundary values. Afterwards the type (light, dark), size, and a centre point for each patch is determined in step 3a. If the centre point lies within the fingerprint boundaries, the algorithm proceeds to drawing the patch into the buffer. This is step 3b (see figure 3.11a). In this step, pixels in distance generated with exponential distribution from the centre point are drawn into the buffer in a distinctive colour (e.g. red or blue). It is randomly chosen if the pixels of the patch will later be in light colour or dark.

When all the patches are drawn into the buffer in a distinctive colour, the final colour of each pixel is determined in step 4 (see figure 3.11b). First, the neighbouring pixels of each pixel in patch are collected from the input image. Then, based upon the selected algorithm, the final pixel's colour is either one of a randomly chosen neighbouring pixel or mean of all it's neighbour's colours. After this, the patches in buffer are blurred in step 5 (see figure 3.11c).

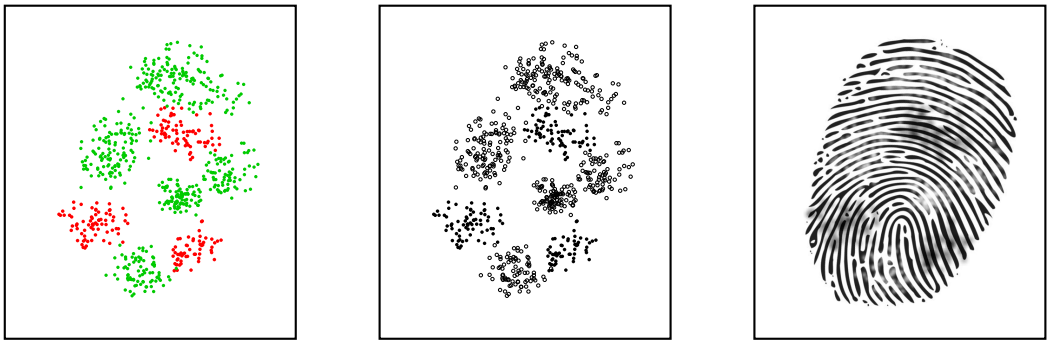

(a) Patches drawn in distinctive colours

(b) Patches drawn in final colours

(c) Blurred patches drawn onto the fingerprint

Figure 3.11: Eczema patches drawing (into buffer) (steps 3, 4, and 5).

The second significant part of the algorithm takes place in step 6 where white lines are drawn into the buffer. Each part of the process is described in the following paragraphs.

In step 6a, parameters of each line are determined. The length of the line is determined within set boundary values and the line direction (either vertical or horizontal) is set. The starting point for line generation is found using random coordinates generation. The starting point must be sufficiently far from all other starting points of all other lines of the same type.

Line points are generated in step 6b. Beginning with the starting point, other leading points are generated based on the length of the line, the direction of the line, and a random generated angle within a pre-defined range (see figure 3.12a).

To make the lines look more realistic, in step 6c, the line leading points count is doubled and spline interpolation of the first order is applied. This makes the line appear less edgy and smooths it (see figure 3.12b).

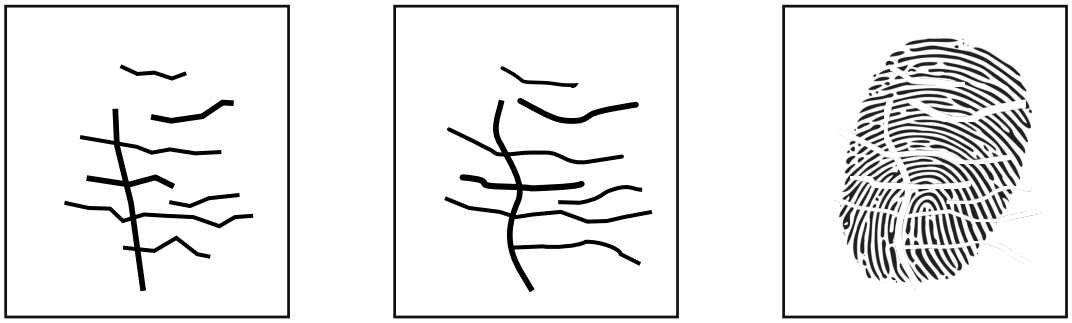

(a) Line leading points

(b) Interpolated line leading points

(c) White lines drawn onto the fingerprint

Figure 3.12: Eczema lines drawing (into buffer) (steps 6b, 6c, and 6d).

Finally, each line is drawn into the buffer in step 6d (see figure 3.12c). The thickness of the line is set and the line is drawn in several steps starting with the whole length drawn in the smallest thickness. Then the first and last leading points are removed and the line is drawn over with a higher thickness. This process repeats until the final set thickness is reached. This ensures that the line's width decreases towards line ends.

In the last two steps, the buffer is once again blurred in step 7 and then in the following step 8, the buffer is drawn into the original fingerprint image taking in consideration the transparency of the pixels in the buffer and blending them into the original image appropriately.

Chapter 4

Disease-simulating methods implementation and results

This chapter explains the decisions taken in a process of implementing the methods for simulating previously described diseases in synthetic fingerprint images.

Implementation tools, the environment and techniques used are described in the following section 4.1 in detail. The implemented solution description of a fingerprint disease simulator follows next in section 4.2 with the fundamental parts of all the application classes thoroughly described. In the end of this chapter in section 4.3, the resulting fingerprints with simulated diseases of warts and atopic eczema are presented together with the original images for the reader to compare the results achieved.

4.1 Implementation tools and environment

The system for simulating diseases in synthetic fingerprints has been designed as a console application processing an input image and producing an output image with marks of a selected disease. The marks generation process can be customized by various command-line parameters.

The simulator has been implemented in the Python[1] programming language, specifically in version 3.4.0. For the graphic operations, a computer vision library OpenCV[2] in version 3.1 has been extensively used. The library has been used for image file manipulation, 2D drawing, and image processing like thresholding, smoothing or contour detection. Other libraries used include the scientific computing library NumPy[3], on which OpenCV relies heavily, and SciPy[4].

The simulator implementation is multi-platform and should run on all main operating systems without any obstacles. All used libraries are multi-platform as well and no platform-specific code has been used. The application was developed and tested on a PC platform with Xubuntu operating system in version 15.10 installed.

[1] http://www.python.org
[2] http://www.opencv.org
[3] http://www.numpy.org
[4] http://www.scipy.org

4.1.1 SFinGe automation tool

SFinGe, one of the synthetic fingerprint generators described in section 2.5, has been chosen as the input generator for this task. In its freely available version however, it allows generating only one fingerprint at a time and all the parameters of the generation have to be manually specified during the process by the user.

In order to automate the process of generating hundreds of synthetic fingerprint images manually, an automation script has been implemented, making this time-consuming task easier. The automation script has been implemented in Python using a tool for visual-based automation SikuliX[5]. It allows to go through the process of generating a synthetic fingerprint automatically, setting parameters in the SFinGe GUI based on constrains given in the source code of the automation script.

The automation tool is not an official part of the implemented *Fingerprint disease simulator* system. It is provided merely as a tool developed aside from the main thesis goal in hope that it might be of use to others.

4.2 Fingerprint disease simulator

Fingerprint disease simulator, the thesis product, has been implemented with modular design and extendibility in mind. Using an object-oriented programming approach, a main base class representing a single disease generator has been implemented. It has been named `BaseGenerator` and implements common methods for all specific disease generator classes.

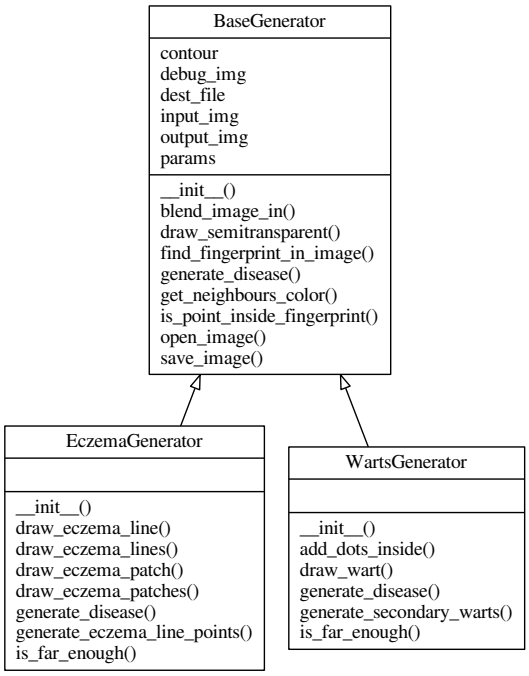

Figure 4.1: Class diagram of the Fingerprint disease simulator.

[5] http://www.sikulix.com

Two generator classes extending the `BaseGenerator` have been implemented. `WartsGenerator` class implements designed methods for damaging the synthetic fingerprint with warts. Likewise, `EczemaGenerator` class implements methods of simulating atopic eczema in a synthetic fingerprint image. Implementation details of the generator classes can be found in the following paragraphs. A class diagram of the implemented solution can be seen in figure 4.1.

The entry point to the application is `main.py` file. Its primary task is parsing command-line arguments and passing them as parameters to the disease generator objects. The generator to be used is chosen based on a `--type` argument. A detailed description of all available command-line arguments can be found in the application manual on the DVD attached.

4.2.1 BaseGenerator class

The `BaseGenerator` class is the core of the *Fingerprint disease simulator* application. It serves as a base class for all specific disease generators and provides shared convenience methods to be used by them. It also defines an interface for other specific generators to implement. This allows the implemented application to be easily extended by adding new modules generating other diseases into synthetic fingerprints.

All specific disease generators share the `__init__()` method which initializes the generator object as well as defines important object variables. Parameters are extracted from the command line argument parser and according to their values, the input image is opened and loaded using the `imread()` method provided by the OpenCV library, the output image is created as a copy of the input image, and optionally in case that the debugging is enabled, the debug image is created in a similar fashion.

In the next step of the initialization process, the fingerprint is found on the input image. In order to do that, the `find_fingerprint_in_image()` method is called. First the input image is binarized using adaptive thresholding provided by OpenCV and then it is blurred using the Gaussian blurring method with kernel of size 11×11 and $\sigma = 5$. This allows the algorithm to use a contour-finding method more efficiently. The contour area of all contours found is then computed and the largest one is returned as the contour of the fingerprint.

Other shared methods provided by the `BaseGenerator` class include helping method `is_point_inside_fingerprint()` which, using an OpenCV method `pointPolygonTest()`, determines if the given point is inside of the fingerprint contour or not. Another helping method is called `get_neighbours_color()`. Its task is to find neighbouring pixel colours and return the final colour of the pixel based on the method specified as a parameter of the application. Two other helping methods `blend_image_in()` and `draw_semitransparent()` are used to blend given image buffer pixels with input image seamlessly using the alpha channel value of the image buffer pixels.

The class also provides an abstract method `generate_disease()` which is to be implemented by all specific disease generator classes in order to generate marks into the synthetic fingerprint image.

4.2.2 WartsGenerator class

The `WartsGenerator` class is an implementation of warts fingerprint marks generator for the *Fingerprint disease simulator* application. As all specific disease generators, it extends the `BaseGenerator` class.

After the generator is initialized, the `generate_disease()` method is called. Inside of this method, the marks of warts are generated into the synthetic fingerprint image. First, a random coordinates of a point inside of the fingerprint contour are found. This is the new centre of the wart to be generated. With the wart's size determined by generating a random value within set boundary values, `draw_wart()` method is called.

Within the `draw_wart()` method, an image buffer large enough for the newly generated wart to fit in is created. Then the main part of the warts-generating process takes place in this method. First, a number of small circles is generated and stored in a list. Each of the circle is defined by its radius and a centre point. The centre point is determined by a calculation of coordinates using a randomly generated angle α and a randomly generated radius r. Using a simple equation 4.1, the centre point $[x_{circle}, y_{circle}]$ of a new circle is calculated:

$$\begin{aligned} x_{circle} &= x_{centre} + r \cdot \cos\alpha \\ y_{circle} &= y_{centre} + r \cdot \sin\alpha, \end{aligned} \tag{4.1}$$

where $[x_{centre}, y_{centre}]$ is the wart's centre point. The drawing of the generated small circles is then done in two steps. First, the circles are drawn in a distinctive colour representing the outline of the circles. Afterwards, the same circles are drawn only with their radius smaller by one to two pixels. This creates a desired effect of a wart composed of a number of small circles with only the outline of the whole wart object visible. This is better illustrated by figure 4.2a, which represents an actual output of the implemented algorithm.

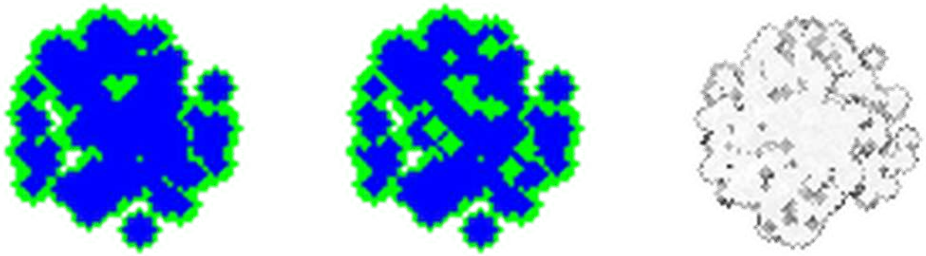

(a) Wart drawing: circles (b) Wart drawing: dark dots (c) Wart drawing: pixel colouring

Figure 4.2: Process of wart drawing into an image buffer (enlarged).

The next step in wart simulation is adding black dots inside of the wart. This is done in `add_dots_inside()` method call. The coordinates of the dark dot centre are randomly generated. If the colour of the pixel on the generated coordinates is the inner colour of the wart, a circle of a small radius (one to two pixels) is drawn in the colour of the wart's border. The result of the process can be seen on figure 4.2b.

The wart drawing process continues by executing a common method `blend_image_in()` which changes colours of pixels drawn in distinctive colours to better match the fingerprint colour scheme (see figure 4.2c). Blurring of the wart with kernel of size 3×3 in image buffer follows, making the image less sharp and look more realistic. After that, the buffer is drawn into the output image with respect to the alpha channel value of each pixel. This is done using a common method `draw_semitransparent()` from the `BaseGenerator` class. The result can be seen on figure 4.3a.

(a) Main wart drawing (b) Secondary wart drawing

Figure 4.3: Wart drawing process.

An optional part of the wart drawing process is generation of the secondary warts. The method responsible for secondary warts drawing is called `generate_secondary_warts()`. As a default, secondary warts drawing happens only with a 50% chance and the maximum number of them can be set as a parameter of the application. The process of secondary warts drawing is the same as with the main wart except the algorithm furthermore checks the minimal distance from the other secondary warts so that they do not overlap. For this, a helping method `is_far_enough()` is called. The final output of the algorithm is represented by figure 4.3b.

4.2.3 EczemaGenerator class

The second of implemented generators for the *Fingerprint disease simulator* is the `Eczema-Generator` which simulates marks of atopic eczema into a synthetic fingerprint. It also extends the `BaseGenerator` class.

After the generator is initialized, the `generate_disease()` method is called. Inside of this method, the marks of atopic eczema are generated into the synthetic fingerprint image. First, an image buffer of the same size as the input image is created.

Next, the eczema colour patches are drawn into the synthetic fingerprint image. For this, the `draw_eczema_patches()` method is responsible. The number of colour patches to generate is determined randomly within bounds set by arguments passed to the application. For each patch, its colour is determined first. It is either a dark or white patch. Then a centre point of the patch is randomly generated within the fingerprint contour along with the radius of the patch.

The drawing of the patches itself does the `draw_eczema_patch()` method. Within the method, a number of points around the centre point are created. The distance of the points from the centre point is generated with exponential distribution. Using a similar equation as equation 4.1, the point coordinates are calculated. If the point is within the boundaries of the fingerprint, a small circle with radius of 1 pixel is drawn into the image buffer (see

figure 4.4a).

The pixels of the patches are then drawn with appropriate colours that fit the fingerprint image by using the `blend_image_in()` common method. Afterwards, the image buffer is blurred using the OpenCV `blur()` method with kernel of size 3×3. After these steps, the result can be seen on figure 4.4b.

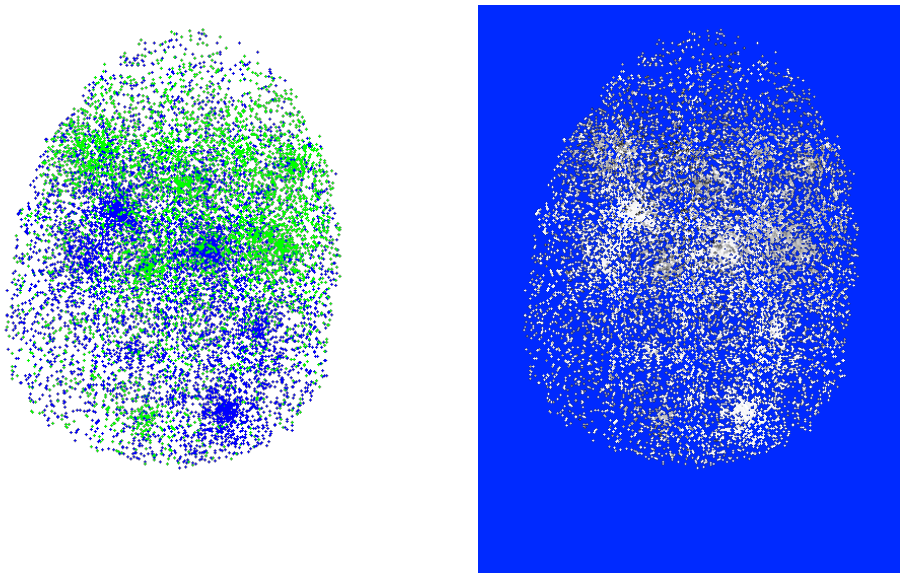

(a) Patches drawn in distinctive colours

(b) Final patches drawing (background is added for better visibility)

Figure 4.4: Atopic eczema patches drawing process.

Another specific mark for atopic eczema are white lines running throughout the whole fingerprint. These are simulated inside of the `draw_eczema_lines()` method call. The lines can be either of a horizontal or vertical direction and the two types are generated separately.

For each generated line, the starting point is first found with its coordinates generated randomly within the fingerprint contour boundaries. Also, the minimal distance from all starting points of other already generated lines is checked. If a valid starting point is found, the length of the line to be generated is determined within boundary values set.

Line leading points are generated by the `generate_eczema_line_points()` method. Within this method, the direction of the generating is determined randomly (left or right for horizontal lines; up or down for vertical lines). Each following point is generated using a similar equation as equation 4.1. The angle is generated randomly within boundaries set and depending on the type of the line (horizontal or vertical) and its direction.

The generated leading points of each line are afterwards interpolated using a SciPy interpolation method `interp1d()` with linear spline interpolation algorithm. Then the line is drawn into the image buffer using the `draw_eczema_line()` method which internally uses the OpenCV `polylines()` method.

In order to make the line look realistic, it is drawn with its width thinner towards its ends. This effect is achieved by drawing the full line in the lowest width and gradually drawing thicker lines without the first and the last leading points over the previous ones (see figure 4.5a).

The pixels of the lines are then drawn in white colour to fit in the fingerprint image by using the `blend_image_in()` common method. Afterwards the image buffer is blurred once again using the OpenCV `blur()` method with kernel of size 3×3. The simulated atopic eczema lines at this point of the process can be seen on figure 4.5b.

As the last step, the buffer pixels are drawn into the output image with respect to their alpha channel value using the `draw_semitransparent()` common method.

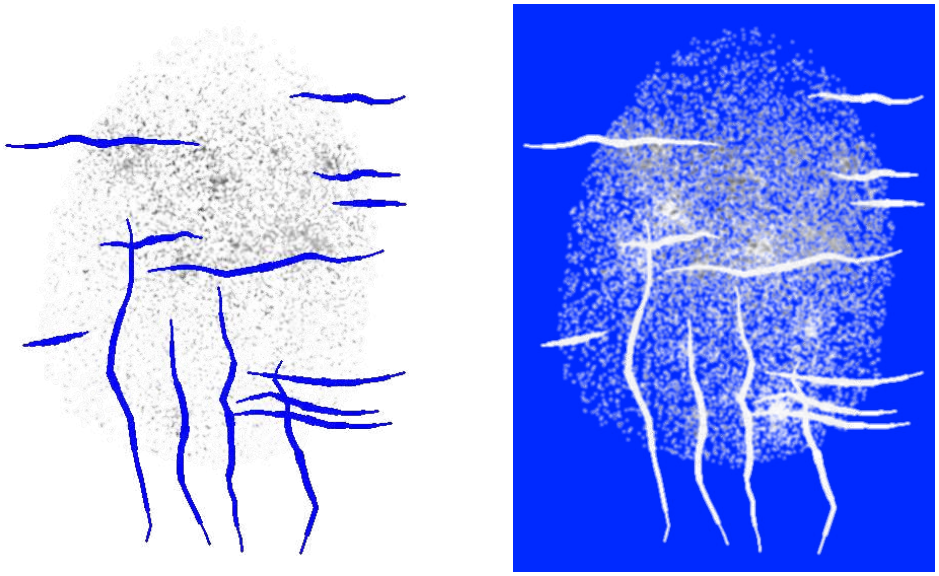

(a) Lines drawn in distinctive colours

(b) Final lines drawing (background is added for better visibility)

Figure 4.5: Atopic eczema lines drawing process.

4.3 Implementation results

Example result outputs of warts generator and atopic eczema generator by the *Fingerprint disease generator* are presented in this section. Selected samples of original fingerprints from the STRaDe database with similar disease marks are presented alongside for comparison. For the complete set of generated fingerprints, please refer to the attached DVD.

4.3.1 Warts simulation results

Figure 4.6 shows two selected samples of fingerprints affected by warts taken from the STRaDe database.

The following figure 4.7 represents two selected sets of fingerprint images to show the product of fingerprint disease simulation. Subfigures 4.7a and 4.7c represent original synthetic fingerprints and next to each of them, on subfigures 4.7b and 4.7d, there are the same images with disease marks on them implemented by the *Fingerprint disease simulator*.

The parameters of the fingerprint disease simulator used for simulating the disease marks into the synthetic fingerprint images have been kept to default (for more information, please refer to the application manual on the attached DVD).

(a) (b)

Figure 4.6: Samples of original warts-affected fingerprint from the STRaDe database.

(a) Synthetic fingerprint (b) Warts simulation result

(c) Synthetic fingerprint (d) Warts simulation result

Figure 4.7: Fingerprint warts simulation results.

4.3.2 Atopic eczema simulation results

Figure 4.8 shows two selected samples of fingerprints affected by warts taken from the STRaDe database.

(a) (b)

Figure 4.8: Samples of original eczema-affected fingerprint from the STRaDe database.

The following figures 4.9 and 4.10 represent two selected sets of fingerprint images to show the product of fingerprint disease simulation. Subfigures 4.9a and 4.10a represent the original synthetic fingerprints. On the right from each of them, the same images with disease marks on them implemented by the *Fingerprint disease simulator* can be seen (subfigures 4.9b and 4.10b).

The parameters of the fingerprint disease simulator used for simulating the disease marks into the synthetic fingerprint images have been kept to default (for more information, please refer to the application manual on the attached DVD).

(a) Synthetic fingerprint (b) Eczema simulation result

Figure 4.9: Fingerprint atopic eczema simulation results.

(a) Synthetic fingerprint (b) Eczema simulation result

Figure 4.10: Fingerprint atopic eczema simulation results.

Chapter 5

Fingerprint verification and quality assessment

In order to evaluate the output of the *Fingerprint disease simulator*, the resulting damaged fingerprints must undergo verification against unmodified synthetic fingerprint images and their quality has to be measured. Thirteen sets, each containing 250 fingerprint images have been generated with different parameters for evaluation. A detailed description of the datasets can be found in section 5.1.

Two methods of evaluation have been selected. *VeriFinger*[1] by NEUROtechnology has been used for the fingerprint verification. The output is a matching score of a damaged fingerprint expressed in a relation to a matching score of the original fingerprint that has been verified against itself. The results for both warts datasets and eczema datasets can be found in section 5.2.

NFIQ 2.0[2] fingerprint quality assessment tool has been used to determine the quality of the damaged fingerprints compared to the quality of unmodified synthetic fingerprints. The output is a score based on several quality features computed from the fingerprint image. The results for the warts and eczema datasets are presented in section 5.3 in detail.

Due to the large size of each dataset, only results evaluated for the whole dataset are presented, usually in form of median values. For the full results set, please refer to data on the DVD attached.

5.1 Description of datasets

For the purpose of verification and quality assessment of the synthetic fingerprints with disease marks generated by the *Fingerprint disease simulator*, a total number of thirteen datasets have been generated, each containing 250 unique fingerprint images affected by warts or atopic eczema. Each dataset has been created with different set of parameters of the algorithm so that it can be evaluated which parameters affect the quality of the fingerprint the most.

The parameters of warts datasets are presented in table 5.1. Four datasets of warts-affected fingerprints have been created in total. Warts dataset 1 and 2 are generated with warts size set to 5–10% of hypothetical radius of the fingerprint, while the size for dataset 3 and 4 is set to 10–15%. The maximum number of secondary warts *(Max. SW cnt)* is two for datasets 2 and 4. In case of datasets 1 and 3, they have been disabled completely.

[1] http://www.neurotechnology.com/verifinger.html
[2] http://www.nist.gov/itl/iad/ig/development_nfiq_2.cfm

Dataset	Wart size [%]	Max. SW cnt
Warts 1	5–10	0
Warts 2	5–10	2
Warts 3	10–15	0
Warts 4	10–15	2

Table 5.1: Warts datasets parameters.

The number of eczema datasets generated for verification and quality assessment is nine and the parameters for each dataset can be found in table 5.2. The parameters include range of horizontal white lines count *(HL cnt)*, vertical lines count *(VL cnt)*, line length represented by percentage of hypothetical fingerprint radius *(L. length)*, line width *(L. width)*, patches count *(P. cnt)* and their size in percent relative to hypothetical fingerprint radius *(P. size)*.

Datasets 1–4 combine different line types and their length, while eczema datasets 5 and 6 add different line thickness. Datasets 7 and 8 contain different amount of patches with no lines and the last dataset 9 combines the vertical and horizontal lines with patches together.

Dataset	HL cnt	VL cnt	L. length [%]	L. width	P. cnt	P. size [%]
Eczema 1	4–12	0	50–100	8	0	0
Eczema 2	4–12	0	100–200	8	0	0
Eczema 3	0	2–6	50–100	8	0	0
Eczema 4	0	2–6	100–200	8	0	0
Eczema 5	4–12	2–6	50–200	8	0	0
Eczema 6	4–12	2–6	50–200	5	0	0
Eczema 7	0	0	0	0	2–10	20–80
Eczema 8	0	0	0	0	10–20	20–80
Eczema 9	4–12	2–6	50–200	8	4–20	20–80

Table 5.2: Eczema datasets parameters.

5.2 NEUROtechnology VeriFinger

For verification of generated disease-affected fingerprint, *VeriFinger*, a fingerprint identification tool by NEUROtechnology, has been used.

The tool allows the user to enroll fingerprints into a database and verify or identify fingerprints against the existing database templates. During the process, a matching score is printed out. This score has been used to evaluate the degree of the damage generated by the *Fingerprint disease simulator* into the synthetic fingerprint.

The methodology of the verification process is as follows:

1. enroll the original unmodified synthetic fingerprints into the database;
2. verify the same unmodified synthetic fingerprints and save their scores (this constitutes a baseline score — 100% score);

3. for each fingerprint from a given testing set, verify the damaged fingerprint against the original unmodified one and record the matching score;
4. evaluate the percent value of the recorded matching score — the normalized median value of the matching score;
5. calculate the median value for each set.

5.2.1 Warts

The results of warts-affected fingerprint verification are presented in table 5.3. The table contains the median of the set matching score as well as its normalized value. Graphical representation of the result values can be found on figure 5.1.

Dataset	**Original**	**Warts 1**	**Warts 2**	**Warts 3**	**Warts 4**
Median	1116.50	1037.50	1029.00	944.50	918.00
Norm. median [%]	100.00	93.47	92.74	85.80	83.42

Table 5.3: VeriFinger score: warts datasets.

From the data in table 5.3 it is clear that presence of warts in a fingerprint negatively affects the value of the fingerprint matching score. The *Warts 1* and *Warts 2* datasets are generated with only relatively small warts in size, while the other two datasets, *Warts 3* and *Warts 4* contain noticeably larger warts. Because of this, the score dropped by almost 10% when warts were relatively small (size parameters set to 5–10%) and by about 15% for larger warts (size parameter set to 10–15%).

Also the presence of secondary warts in datasets *Warts 2* and *Warts 4* lowers the final score considerably (by 0.73% in case of *Warts 1* compared to *Warts 2*; and by 2.38% for *Warts 3* and *Warts 4* datasets).

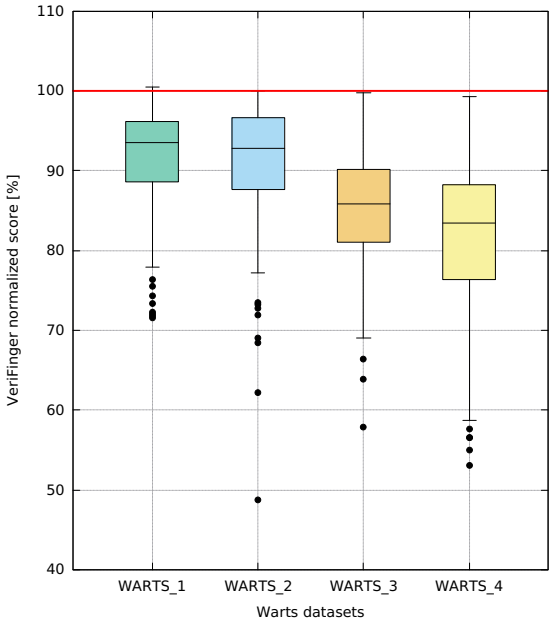

Figure 5.1: VeriFinger score: warts datasets.

The most probable reason for this is that the wart in a fingerprint creates new minutiae while covering those present before the disease has been generated into the fingerprint. This results in lower matching score as some ridge structures cannot be properly matched by the algorithm any more.

5.2.2 Atopic eczema

The results of atopic eczema-affected fingerprint verification are presented in table 5.4. The table contains the median of the set matching score as well as its normalized value. Graphical representation of the results can be found on figure 5.2.

Dataset	**Original**	**Ecz. 1**	**Ecz. 2**	**Ecz. 3**	**Ecz. 4**
Median	1116.50	836.50	841.50	855.50	857.50
Norm. median [%]	100.00	76.11	75.94	77.15	77.80

Dataset	**Ecz. 5**	**Ecz. 6**	**Ecz. 7**	**Ecz. 8**	**Ecz. 9**
Median	809.00	869.50	842.00	761.50	706.00
Norm. median [%]	73.79	78.33	76.25	68.20	64.30

Table 5.4: VeriFinger score: eczema datasets.

Judging from the data acquired, when comparing datasets *Eczema 1* and *Eczema 2* with datasets *Eczema 3* and *Eczema 4*, it can be said that the type of eczema lines on the fingerprint has only little effect on the matching score (approximately 24% decrease for horizontal lines versus circa 23% decrease). The damage caused by the horizontal and vertical lines is principally the same. The white lines disrupt the flow of ridges and thus create new false minutiae in places of line crossing.

The length of the lines has a negligible effect on the final matching score. The difference of medians of datasets *Eczema 1* and *Eczema 2* is only 0.17% and in case of datasets *Eczema 3* and *Eczema 4*, the difference is 0.65%.

The small difference might be caused by the fact that a significant part of the line can be generated outside of the fingerprint. The reason for this is that while the starting point of the line is generated to be inside of the fingerprint, the direction of line generating is decided randomly. Therefore if the starting point is located near the fingerprint border and the direction is determined to point out of the fingerprint, the generated line might be in fact shorter than expected.

Examining the influence of line thickness on the matching score by comparing datasets *Eczema 5* and *Eczema 6* shows that thicker lines have a greater damaging effect on the fingerprint. The median of matching score for lines of maximal thickness 8 is only 73.79%, while the median of score for lines of maximal thickness 5 is 78.33%. This effect can be explained by the fact that thinner ridge disruptions might be repaired by the matching algorithm, while thicker lines discontinue the ridges more effectively.

Comparing each single eczema damage type (white lines versus patches), the one causing the greatest damage to the fingerprint are patches. Their effect is most significant when a large amount of patches is generated into the fingerprint. Compare dataset *Eczema 7* (2–10 patches per fingerprint) with median of matching score 76.25% versus dataset *Eczema 8* (10–20 patches per fingerprint) with median of matching score 68.20%. The patches in

fingerprint make the ridge structure effectively less clear and bring more noise into it. This makes the minutiae recognition process for the matching algorithm harder to do, thus lowering the matching score.

The most effective damaging results are brought by both types of damage (white lines and patches) combined. As represented by dataset *Eczema 9*, the median of matching score declined to 64.30%.

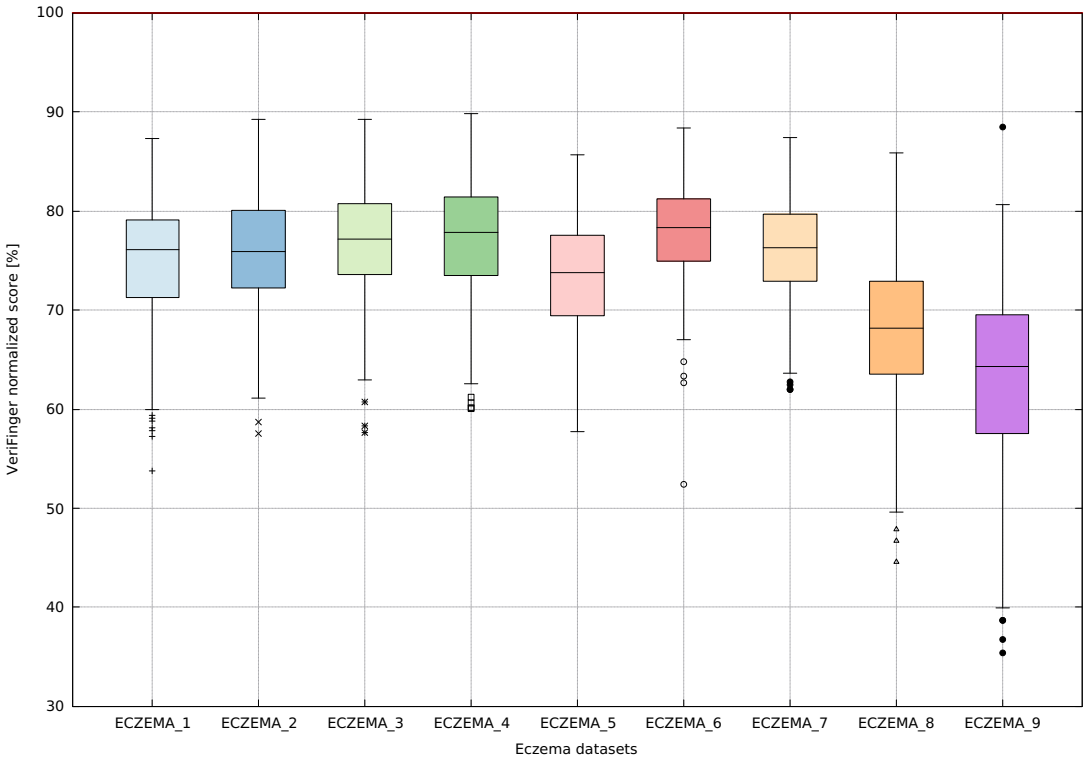

Figure 5.2: VeriFinger score: eczema datasets.

5.3 NIST NFIQ 2.0

The second method of damage verification caused to synthetic fingerprint by the *Fingerprint disease simulator* has been done with the help of *NFIQ 2.0* fingerprint quality assessment tool released by the NIST (National Institute of Standards and Technology).

In order to assess the quality of a fingerprint, NFIQ 2.0 computes a set of quality features from the input image, and uses them to predict the fingerprint image quality. The output of the algorithm is a score value in range of [0–100], where 0 represents an image of no utility and 100 is the highest utility value. The NFIQ 2.0 algorithm bases its score computation on fourteen selected quality features which together constitute the final score for given input image.

The base score has been established for each fingerprint by evaluating the quality of the unmodified original synthetic fingerprint image. Then for each damaged fingerprint, its score has been evaluated. A median of scores for each dataset has been found and expressed in percent in relation to the base score median.

5.3.1 Warts

The results of warts-affected fingerprint quality assessment can be seen in table 5.5. The table contains the median of set quality score as well as its normalized value. Graphical representation of the result values can be found on figure 5.3.

Dataset	Original	Warts 1	Warts 2	Warts 3	Warts 4
Median	64.00	66.00	66.00	67.00	67.00
Norm. median [%]	100.00	101.92	101.92	104.20	104.20

Table 5.5: NFIQ2 score: warts datasets.

As data in table 5.5 shows, the NFIQ2 score actually increased for all testing datasets of warts-affected fingerprints when compared to the unmodified original synthetic fingerprint dataset.

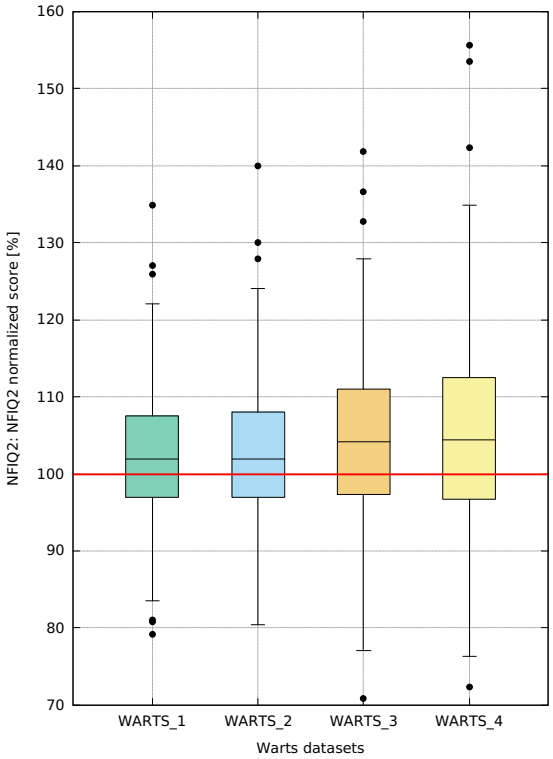

Figure 5.3: NFIQ2 score: warts datasets.

In order to explain this, the NFIQ2 score calculation has to be taken into account. The value of the score is based on fourteen different quality features computed from the input fingerprint image. Because the application decision logic is based on a trained random forest learning, not all quality features have the same weight. Detailed information on the weight of each quality feature can be found in the NFIQ 2.0 documentation[3] (page 29).

Therefore, it can be assumed that the quality features affected by changes implemented by the *Fingerprint disease simulator* do not have weight large enough to influence the final

[3] http://biometrics.nist.gov/cs_links/quality/NFIQ_2/nfiq2_report.pdf

NFIQ2 score. In fact, as in this case, some other quality features might be enhanced by the changes so that the final score rises above the score of the control set.

Detailed examination of several individual quality feature results can be found in section 5.3.3 further down.

5.3.2 Atopic eczema

Quality assessment results of fingerprints affected by atopic eczema can be found in table 5.6. The table contains the median of set quality score as well as its normalized value. Graphical representation of the result values can be found on figure 5.4.

Dataset	**Original**	**Ecz. 1**	**Ecz. 2**	**Ecz. 3**	**Ecz. 4**
Median	64.00	65.00	64.00	63.00	64.00
Norm. median [%]	100.00	101.71	100.00	100.00	100.00

Dataset	**Ecz. 5**	**Ecz. 6**	**Ecz. 7**	**Ecz. 8**	**Ecz. 9**
Median	66.00	64.00	65.00	68.00	68.00
Norm. median [%]	102.03	100.00	101.79	104.67	104.67

Table 5.6: NFIQ2 score: eczema datasets.

Also in the case of eczema datasets, the NFIQ2 quality score is equal or higher than the score of the control dataset. The reasons have been described in previous section and are the same in this case also.

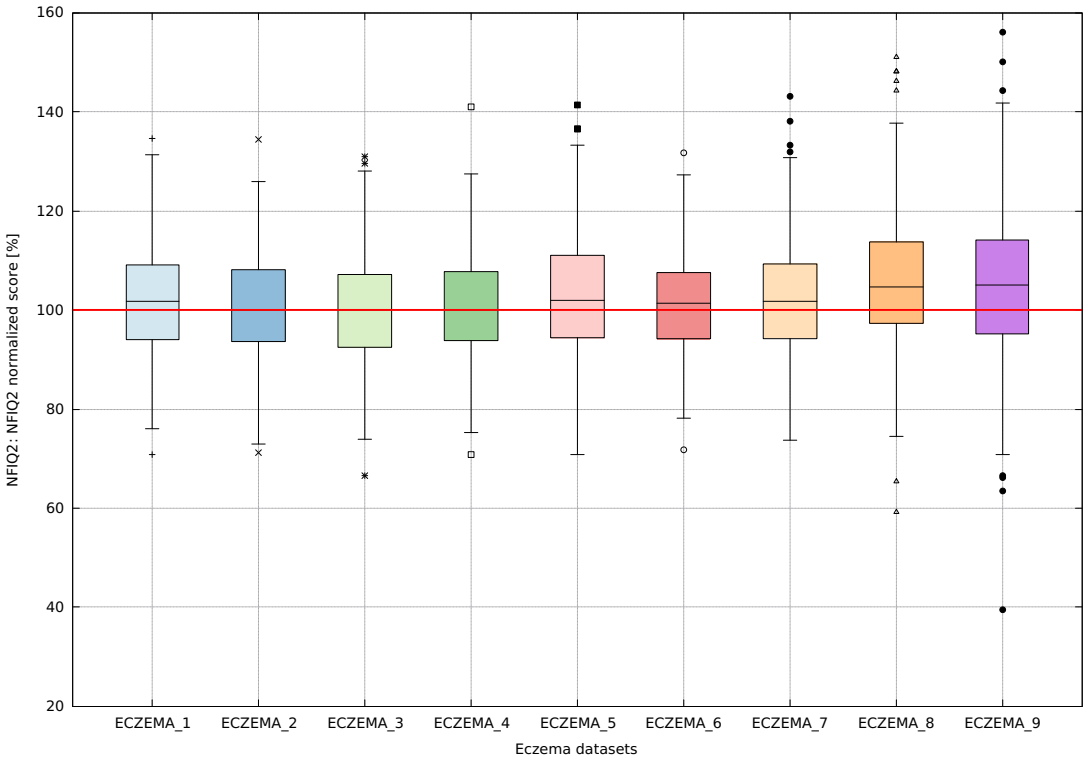

Figure 5.4: NFIQ2 score: eczema datasets.

5.3.3 NIST NFIQ 2.0: selected quality features

In order to explain the higher value of NFIQ2 score for all datasets of damaged fingerprints, while the exact opposite was expected, the NFIQ2 score computation method has to be studied. The score value is calculated from fourteen unique quality features of a given fingerprint. The predicted value is determined by an implementation of random forest algorithm that has been trained on existing testing fingerprint datasets.

Therefore, not all the quality features have the same weight when evaluating the quality of given input image. Thus, in order to verify that the changes made by the *Fingerprint disease simulator* bring significant damage marks into the fingerprint, let us investigate the scores of several selected quality features evaluated by the NFIQ 2.0 algorithm. Only quality features that expressed a noticeable change in the score have been selected into the set of examined quality features. Others stayed rather constant when compared to control dataset of unmodified synthetic fingerprints, therefore there is no need to study them further. For the complete results please refer to the contents of the attached DVD.

The NFIQ 2.0 employs a customized version of *FingerJet FX OSE minutia extractor*[4] for determining the count of minutiae detected in the whole image *(Minutiae cnt)* and an arithmetic mean of all minutiae quality values. Two different methods for computing the quality of the minutiae are used.

The first method calculates the quality using an arithmetic mean of pixel values in the input image *(MU M. Quality)*. The second method of minutiae quality assessment computes the quality as the *Orientation Certainty Level* of blocks of pixels centred at the minutia location *(OCL M. Quality)*.

The other quality features presented are *ROI Relative Orientation Map Coherence Sum (OM Coherence)* which represents the average coherence values over all image blocks in the fingerprint ROI.

The last of the studied quality features is the *Ridge Valley Uniformity (Uniform Image)* feature. It measures the consistency of the ridge and valley widths. For a finger image with clear ridge and valley separation it is expected that the ratio remains rather constant and thus the standard deviation of the ratios is used as an indication of the fingerprint quality.

Warts

The results of selected quality features evaluation of the NFIQ 2.0 algorithm for warts-affected fingerprints datasets are presented in table 5.7.

Dataset	Original	Warts 1	Warts 2	Warts 3	Warts 4
Minutiae cnt	36	38	37	43	45
MU M. Quality [%]	85.00	83.00	84.00	75.00	71.00
OCL M. Quality [%]	77.00	71.00	69.00	60.00	55.00
OM Coherence [%]	75.00	74.00	74.00	73.00	72.00
Uniform Image [%]	53.72	53.49	53.42	53.23	53.06

Table 5.7: NFIQ2: selected quality features: warts datasets.

From the summarized results it can be deduced that changes brought by the *Fingerprint disease simulator* generating warts, increase the number of detected minutiae in a

[4] https://github.com/FingerJetFXOSE/FingerJetFXOSE

fingerprint. This means that the newly detected minutiae must be false ones. Increasing the size of warts also increases the number of new false minutiae.

The quality of minutiae measured by both methods previously described also decreases with increasing size of warts generated. Original quality score values of 85% and 77% go down as low as to 0.71% and 0.55% for dataset *Wart 4* containing generated warts of a large size (10–15%) and secondary warts generating enabled.

As far as *OM Coherence* and *Uniformity of Image* quality features are concerned, their score values differ insignificantly from the original control dataset.

To sum up, for warts-affected fingerprints, new false minutiae are detected by the minutiae extractor and their quality is significantly lower than the quality of minutiae found on the original fingerprint image. Other score values change only negligibly.

Atopic eczema

The results of selected quality features evaluation of the NFIQ 2.0 algorithm for datasets containing fingerprints affected by atopic eczema are presented in table 5.8.

Dataset	**Original**	**Ecz. 1**	**Ecz. 2**	**Ecz. 3**	**Ecz. 4**
Minutiae CNT	36	36	36	36	35
MU M. Quality [%]	85.00	79.00	79.00	82.00	80.00
OCL M. Quality [%]	77.00	75.00	76.00	76.00	76.00
OM Coherence [%]	75.00	75.00	75.00	75.00	75.00
Uniform Image [%]	53.72	49.50	49.66	49.69	49.87

Dataset	**Ecz. 5**	**Ecz. 6**	**Ecz. 7**	**Ecz. 8**	**Ecz. 9**
Minutiae CNT	36	36	36	37	40
MU M. Quality [%]	78.00	82.00	79.00	71.00	68.00
OCL M. Quality [%]	72.00	76.00	69.00	46.00	43.00
OM Coherence [%]	74.00	75.00	73.00	67.00	67.00
Uniform Image [%]	49.00	49.61	43.20	36.70	37.58

Table 5.8: NFIQ2: selected quality features: eczema datasets.

Judging from the summary of results presented, the minutiae count does not change significantly for eczema-affected fingerprints. The only exception for this rule is the last dataset *Eczema 9* which contains fingerprints damaged by all types of available eczema marks. In comparison to the other datasets which keep the same number of detected minutiae as the control dataset, the median value of minutiae detected in dataset *Eczema 9* is 40.

The only considerable quality change of the minutiae of fingerprints affected by eczema can be observed in *Eczema 8* (71% and 46% versus 85% and 77% for the control dataset) and *Eczema 9* datasets (68% and 43% versus 85% and 77% for the control dataset). Other datasets do not show such a significant change in quality. The most probable reason for this is that the last two datasets contain a large number of eczema patches generated into the fingerprints. This decreases the quality of minutiae measured by both of the methods of fingerprint minutiae quality assessment.

As far as *ROI Relative Orientation Map Coherence Sum (OM Coherence)* quality feature

is concerned, the only significant change can be seen in *Eczema 8* and *Eczema 9* datasets (the score of both is 67%). The score of control dataset is 75% and the other dataset scores range between 73% and 75%. Again, this is caused by a large number of eczema patches present in fingerprints contained in *Eczema 8* and *Eczema 9* datasets.

For the *Uniformity of Image* quality feature, the score of patches-containing datasets decreases noticeably while datasets containing fingerprints with eczema lines record only a small decrease in score value (approximately 4% decrease). Even a small number of patches brings the score value down to 43.20% for dataset *Eczema 7*. Larger decrease of the score value can be seen in *Eczema 8* and *Eczema 9* datasets (36.70% and 37.58% versus the control dataset value of 53.72%).

All in all, except for the minutiae count, all other quality features are negatively affected by a large number of eczema patches present in a fingerprint image. On the other hand, eczema lines do not have such a significant effect on the score value of selected quality features.

Chapter 6

Conclusion

The aim of the thesis was to design an algorithm for modifying a synthetic fingerprint image in a way similar to the way a real disease would. In order for the goal to be fulfilled, a number of subjects concerning fingerprint biometry had to be studied. Among the subjects there was fingerprint biometry itself, the sensing technology used for acquiring a fingerprint, and the process of fingerprint recognition. Also several synthetic fingerprint generating algorithms have been studied. Finally, familiarization with a number of skin-affecting diseases has been done in order to better understand the effect they might have on the fingerprint ridge structure.

From the STRaDe database of disease-affected fingerprints, two most common diseases have been selected: *warts* and *atopic eczema*. For each of the disease, further study has been carried out. Based on the samples available from the database, an analysis of selected fingerprint images has been conducted and disease-specific features described. Based on the analysis, design of a method for the specific disease generation has been proposed.

The designed methods have been implemented as modules for the *Fingerprint disease simulator* serving as a base for possible future extensions in form of new modules simulating other diseases into synthetic fingerprint images. Tools implemented for automation of the process of generating the dataset of synthetic fingerprints using SFinGe application has been described together with other tools and libraries used to develop the *Fingerprint disease simulator* application. An example of outputs from the application have been presented in the thesis and the full set of output images is available on the DVD attached.

A significant part of the thesis are experiments conducted in chapter 5. In order to verify the damaging effect caused to the synthetic fingerprints by simulating diseases marks to them, thirteen datasets (four warts and nine eczema datasets) each containing 250 fingerprint images has been generated in total. Each dataset has been created using different parameters so that it could be later examined which parameters affects the fingerprint recognition process in what way. Two methods have been used to verify the fingerprints and assess their quality: *VeriFinger* by NEUROtechnology and *NFIQ 2.0* algorithm by the NIST.

When evaluated with the VeriFinger algorithm, warts datasets showed decrease in the matching score depending on the generated warts size. The score for the dataset of warts with the size parameter set to 10–15% and secondary warts generation enabled went as low as 83.42% of the control dataset score.

Even more significant was the decrease of matching score for datasets of eczema-affected fingerprints. For datasets with fingerprints containing white eczema lines only, the score dropped by approximately 23–24% to 76–77% of the control dataset score. It was also found

that more damaging are thicker lines (score of 78.33% for thickness 5 versus 73.79% for line thickness 8). By far, the most damaging effect on the fingerprint ridge structure have eczema patches. The matching score of datasets generated with the patches enabled dropped to 68.20% of the control group score. When patches and eczema lines were combined, the matching score recorded went down to only 64.30%.

As far as the quality assessment is concerned, the final score of the NFIQ 2.0 quality assessment tool did not reflect changes made by the *Fingerprint disease simulator* as expected. The reason for this is that the final score is computed based on fourteen different quality features, each of them having various weight in the algorithm. Therefore, several specific quality features have been selected instead and their results are discussed further.

For warts datasets, there has been an increase in minutiae count compared to the control dataset (up to 45 versus 36 detected minutiae per fingerprint) meaning that the disease marks simulated by the *Fingerprint disease simulator* create new false minutiae in the fingerprint. Along with that, the quality of minutiae decreased significantly, measured by two different methods (by up to 14 percent points and by up to 22 percent points). Other quality features changed only slightly.

Eczema datasets showed almost no new false minutiae creation (except for the last dataset combining the eczema patches and white lines, where the minutiae count rose to 40 compared to 36 minutiae per fingerprint for the control dataset). However, the quality of the minutiae dropped significantly, mainly in datasets with large number of generated patches. The quality dropped by up to 9 percent points by one measuring and by up to 32 percent points measured by the second method. Also the other two quality features (ROI Relative Orientation Map Coherence Sum and Uniformity of Image) dropped significantly for the datasets with large number of generated patches (from 75% down to 67% for the *OM Coherence* and from 53.72% down to 37.58% for the *Uniformity of Image*).

All in all, the changes to the synthetic fingerprints made by the *Fingerprint disease generator* are well-measurable. In case of warts, the main aspect influencing the damage extent is the size of the generated warts and the amount of them. As far as atopic eczema is concerned, the main influencing aspect is the count of eczema patches, while eczema white lines have lesser effect.

The *Fingerprint disease simulator* has been designed so that it can be extended with new modules simulating other fingerprint diseases than warts and atopic eczema. Having worked with such a tool, matching algorithms could profit from the virtually unlimited amount of fingerprints generated in order to adapt themselves and improve the fingerprint recognition of fingerprints with various diseases.

Bibliography

[1] Asker M. Bazen and Sabih H. Gerez. Systematic methods for the computation of the directional fields and singular points of fingerprints. *IEEE Transactions on Pattern Analysis and Machine Intelligence*, 24(7):905–919, 2002. ISSN 0162-8828.

[2] Raffaele Cappelli. SFinGe: an approach to synthetic fingerprint generation. *International Workshop on Biometric Technologies*, pages 147–154, 2004.

[3] Raffaele Cappelli, Matteo Ferrara, Annalisa Franco, and Davide Maltoni. Fingerprint verification competition 2006. *Biometric Technology Today*, 15(7):7–9, 2007. ISSN 0969-4765.

[4] Raffaele Cappelli, Dario Maio, and Davide Maltoni. Synthetic fingerprint-database generation. In *16th International Conference on Pattern Recognition*, volume 3, pages 744–747. IEEE, 2002. ISBN 0-7695-1695-X.

[5] Radek Chaloupka. *Generátor otisků prstů*. Brno, 2007. Master's thesis. Brno University of Technology, Faculty of Information Technology.

[6] Yi Chen, Geppy Parziale, Eva Diaz-Santana, and Anil K. Jain. 3D touchless fingerprints: compatibility with legacy rolled images. In *Biometrics Symposium: Special Session on Research at the Biometric Consortium Conference*, pages 1–6. IEEE, 2006. ISBN 9781424404865.

[7] Antoinette Ciconte, Jan Campbell, Sepehr Tabrizi, Suzanne Garland, and Robin Marks. Warts are not merely blemishes on the skin: A study on the morbidity associated with having viral cutaneous warts. *Australasian journal of dermatology*, 44(3):169–173, 2003. ISSN 0004-8380.

[8] Martin Drahanský, Michal Doležel, Jaroslav Urbánek, Eva Březinová, and Tai-hoon Kim. Influence of skin diseases on fingerprint recognition. *Journal of biomedicine & biotechnology*, 2012. ISSN 1110-7251.

[9] Martin Drahanský, Filip Orság, and Michal Doležel. *Biometrie*. Computer Press, Brno, 2011. ISBN 978-80-254-8979-6.

[10] Thomas P. Habif. *Clinical Dermatology*. Elsevier Health Sciences, 5$^{\text{th}}$ edition, 2010. ISBN 978-0-7234-3541-9.

[11] Anil K. Jain, Yi Chen, and Meltem Demirkus. Pores and ridges: high-resolution fingerprint matching using level 3 features. *IEEE Transactions on Pattern Analysis and Machine Intelligence*, 29(1):15–27, 2007. ISSN 0162-8828.

[12] Anil K. Jain, Patrick Flynn, and Arun A. Ross. *Handbook of Biometrics*. Springer-Verlag New York, Inc., Secaucus, NJ, USA, 2007. ISBN 038771040X.

[13] Anil K. Jain and David Maltoni. *Handbook of Fingerprint Recognition*. Springer-Verlag New York, Inc., Secaucus, NJ, USA, 2003. ISBN 0387954317.

[14] Anil K. Jain, Salil Prabhakar, and Arun Ross. Fingerprint matching: Data acquisition and performance evaluation. *Dept. of Computer Science, Michigan State Univ., East Lansing, Tech. Rep. MSU-CPS-99–14*, 1999.

[15] William D. James, Timothy G. Berger, and Dirk M. Elston. *Andrew's Diseases of the Skin: Clinical Dermatology*. Elsevier Health Sciences, 11$^{\text{th}}$ edition, 2011. ISBN 978-1-4377-3619-9.

[16] Kalle Karu and Anil K. Jain. Fingerprint classification. *Pattern recognition*, 29(3):389–404, 1996. ISSN 0031-3203.

[17] C. Lee, C. Chang, A. Johar, O. Puwira, and B. Roshidah. Fingerprint changes and verification failure among patients with hand dermatitis. *JAMA Dermatology*, 149(3):294–299, 2013. ISSN 2168-6068.

[18] Salil Prabhakar, Sharath Pankanti, and Anil K. Jain. Biometric recognition: Security and privacy concerns. *IEEE Security & Privacy*, (2):33–42, 2003. ISSN 1540-7993.

[19] Roman Rak, Václav Matyáš, Zdeněk Říha, et al. *Biometrie a identita člověka ve forenzních a komerčních aplikacích*. Grada Publishing, Praha, 2008. ISBN 9788024723655.

[20] Johannes Ring, A. Alomar, T. Bieber, M. Deleuran, A. Fink-Wagner, C. Gelmetti, U. Gieler, J. Lipozencic, T. Luger, et al. Guidelines for treatment of atopic eczema (atopic dermatitis) part I. *Journal of the European Academy of Dermatology and Venereology*, 26(8):1045–1060, 2012. ISSN 0926-9959.

[21] Ulrike Schellhaas, Wolfgang Gerber, Stefan Hammes, and Hans M. Ockenfels. Pulsed dye laser treatment is effective in the treatment of recalcitrant viral warts. *Dermatologic surgery*, 34(1):67–72, 2008. ISSN 1076-0512.

[22] U.S. Congress, Office of Technology Assessment. The FBI fingerprint identification automation program: Issues and options. Technical Report OTA-BP-TCT-84, U.S. Government Printing Office, Washington, DC, November 1991.

[23] Chenyu Wu, Jie Zhou, Zhao-qi Bian, and Gang Rong. Robust crease detection in fingerprint images. In *IEEE Computer Society Conference on Computer Vision and Pattern Recognition*, volume 2, pages 505–510. IEEE, 2003. ISBN 0-7695-1900-8.

[24] Xiongwu Xia and Lawrence O'Gorman. Innovations in fingerprint capture devices. *Pattern Recognition*, 36(2):361–369, 2003. ISSN 0031-3203.

[25] Qijun Zhao, Anil K. Jain, Nicholas G Paulter, and Melissa Taylor. Fingerprint image synthesis based on statistical feature models, 2012. ISBN 978-1-4673-1384-1.

[26] Qijun Zhao, Lei Zhang, David Zhang, and Nan Luo. Direct pore matching for fingerprint recognition. In *Advances in Biometrics*, pages 597–606. Springer, 2009. ISBN 978-1-84628-920-0.